



Gatchina, Russia, August 6 - 10, 2018

*Hadron Structure and QCD:  
from Low to High Energies*

Dedicated to the memory of Lev N. Lipatov



# Recent results from STAR

Grigory Nigmatkulov

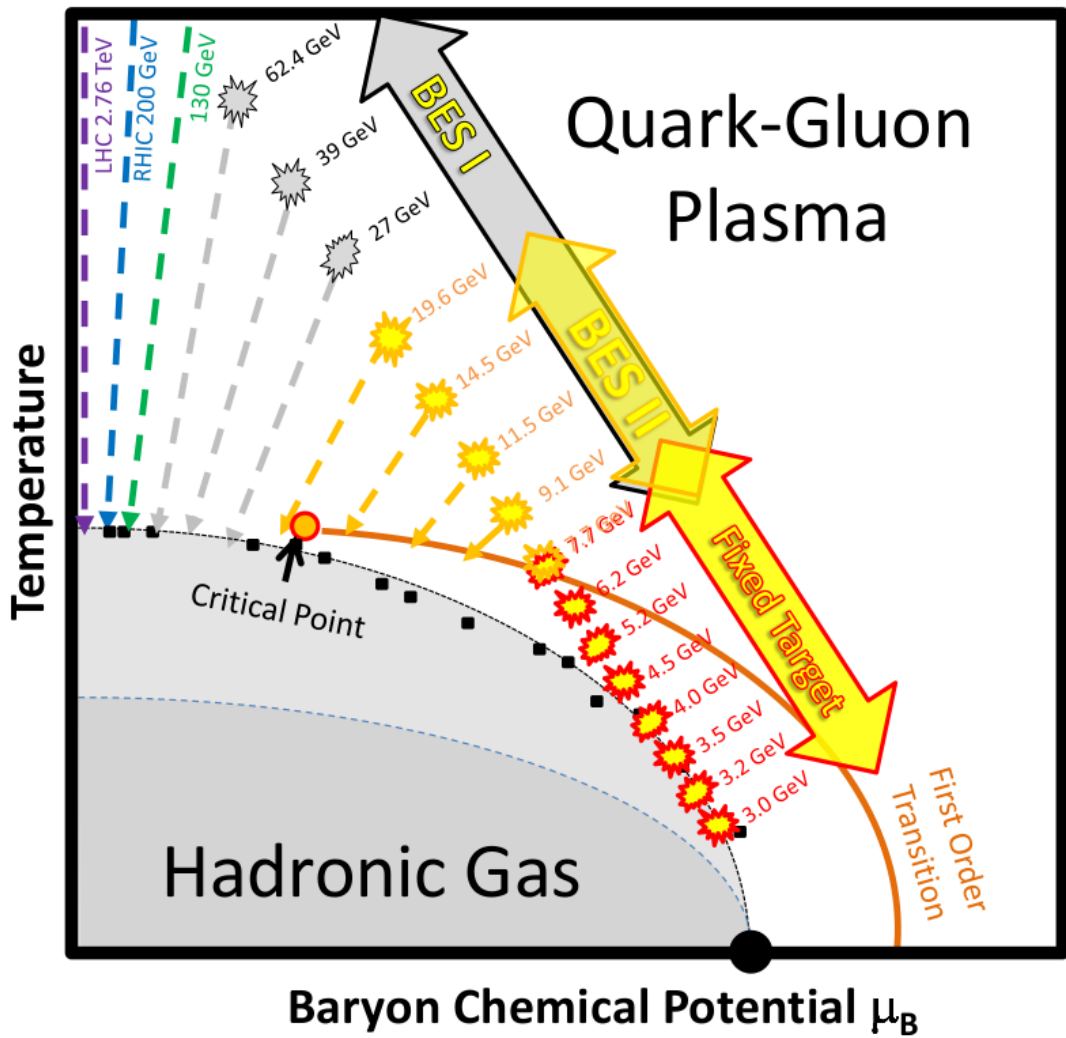
(for the STAR Collaboration)

National Research Nuclear University

MEPhI



- Introduction
- The STAR Experiment
- Collective Dynamics and Correlations
- Particle Production
- High- $p_T$  Hadrons and Jet Modification
- The STAR Fixed-Target Program
- Detector Upgrades
- Summary



**Top RHIC energy**

p+p, p+Al, p+Au, d+Au, <sup>3</sup>He+Au, Cu+Cu, Cu+Au, Ru+Ru, Zr+Zr, Au+Au, U+U

- QCD at high energy density/temperature
- Properties of QGP, Equation of State (EoS)
- Proton spin structure

**Beam Energy Scan**

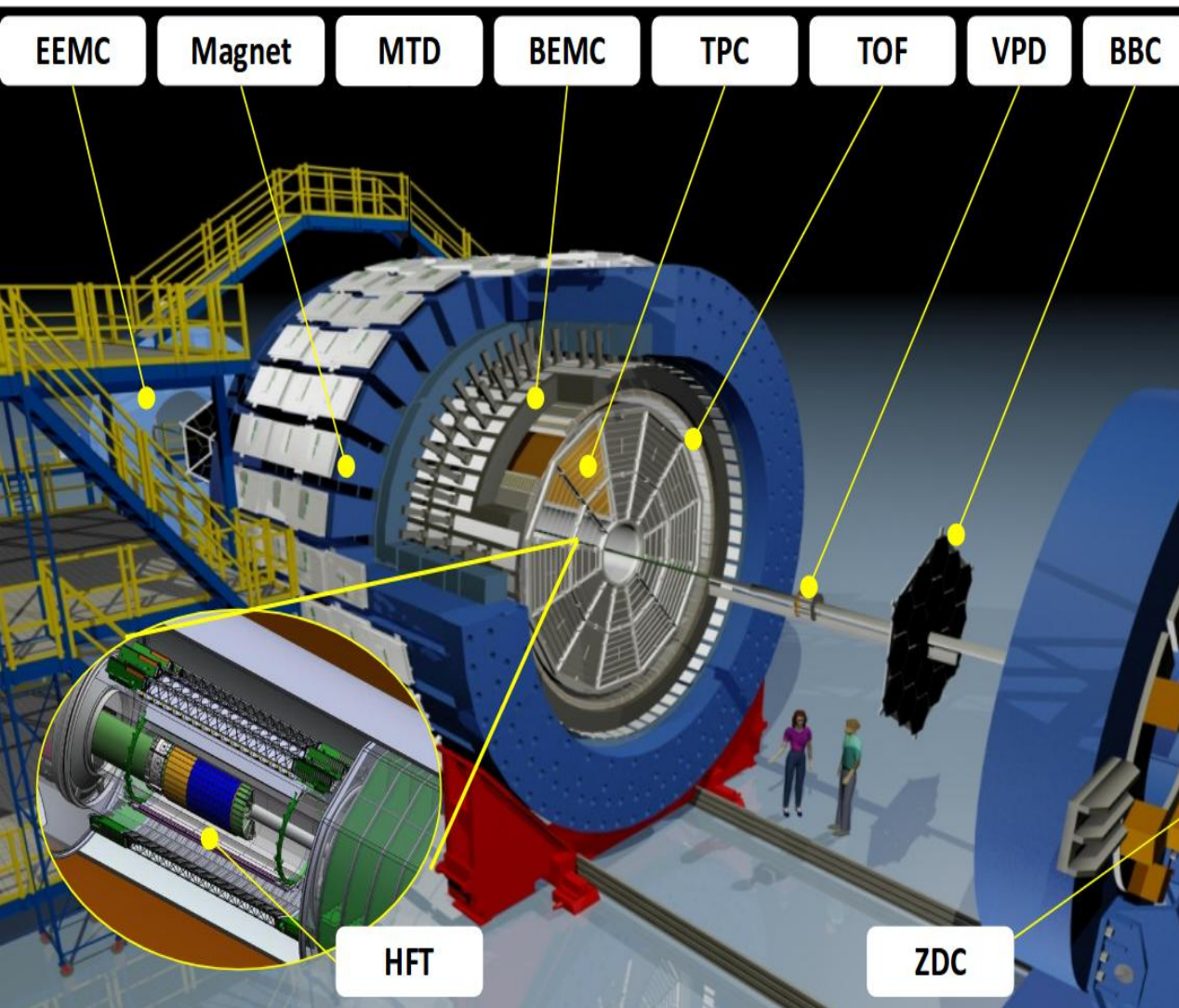
Au+Au  $\sqrt{s_{NN}}=7.7-62.4$  GeV

- Search for critical point
- QCD phase transition
- Turn-off of QGP signatures

**Fixed-Target Program**

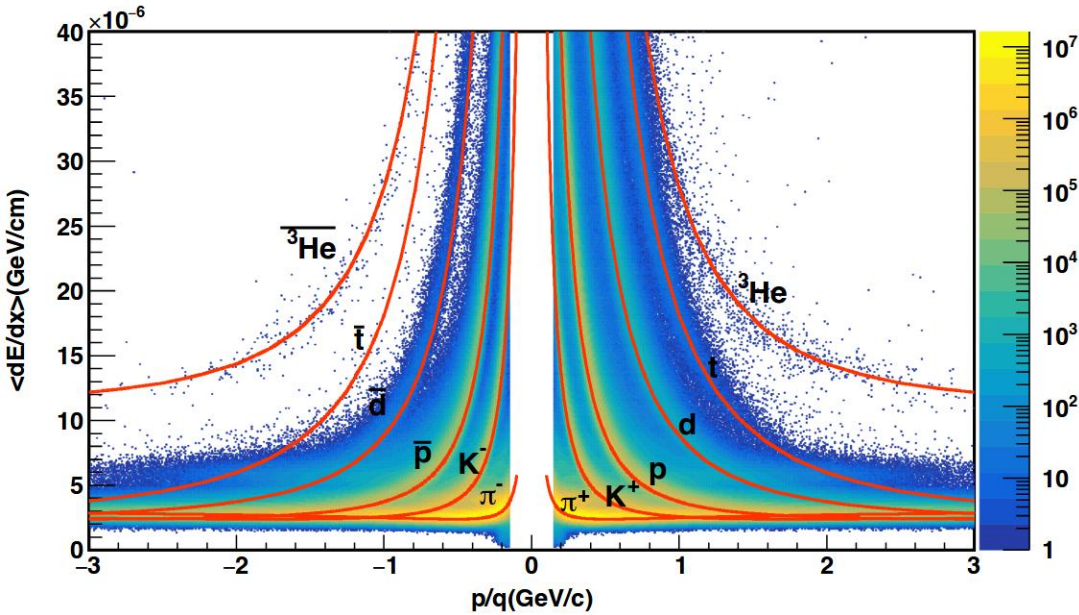
Au+Au  $\sqrt{s_{NN}}=3.0-7.7$  GeV

- High baryon density ( $\mu_B \sim 420-720$  MeV)

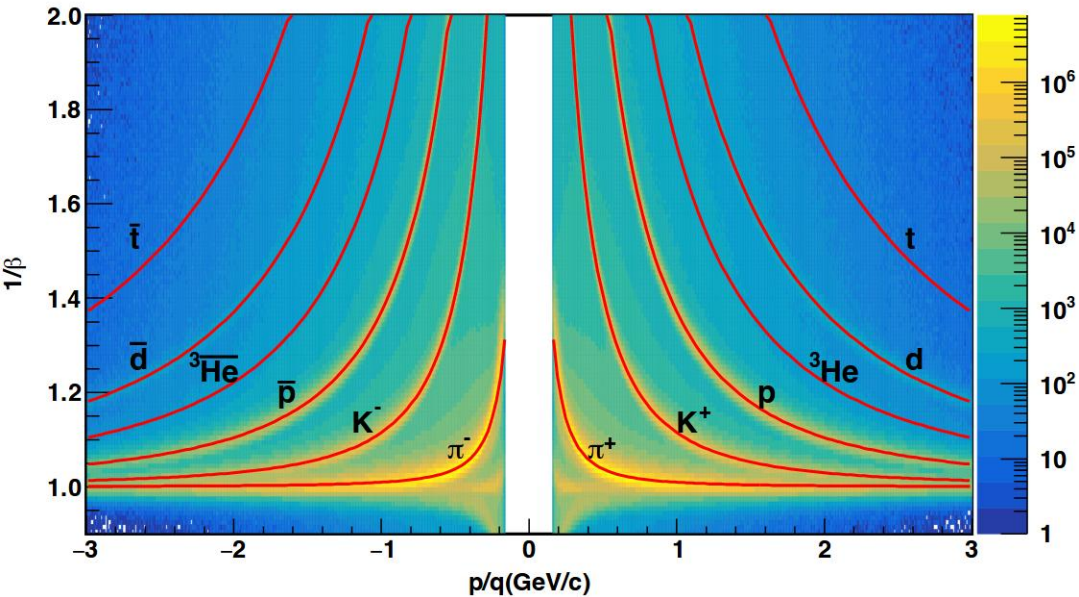


- **Tracking and PID (full  $2\pi$ )**  
 TPC:  $|\eta| < 1$   
 TOF:  $|\eta| < 1$   
 BEMC:  $|\eta| < 1$   
 EEMC:  $1 < |\eta| < 2$   
 HFT (2014-2016):  $|\eta| < 1$   
 MTD (2014+):  $|\eta| < 0.5$
- **MB trigger and event plane reconstruction**  
 BBC:  $3.3 < |\eta| < 5$   
**EPD (2018+):  $3.1 < |\eta| < 5.1$**   
 FMS:  $2.5 < |\eta| < 4$   
 VPD:  $4.2 < |\eta| < 5$   
 ZDC:  $6.5 < |\eta| < 7.5$
- **On-going/future upgrades**  
**iTPC (2019+):  $|\eta| < 1.5$**   
**eTOF (2019+):  $-1.6 < \eta < -1$**   
**FCS (2021+):  $2.5 < \eta < 4$**   
**FTS (2021+):  $2.5 < \eta < 4$**

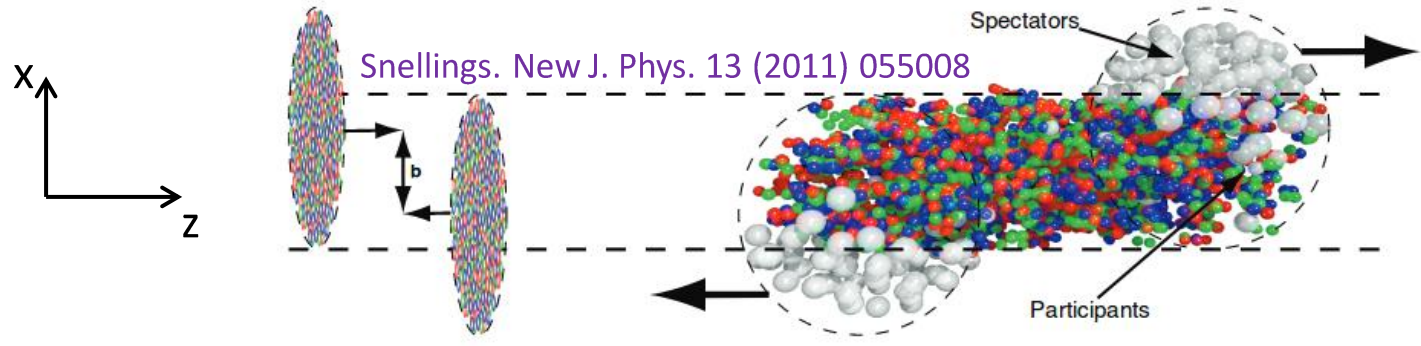




- The  $\langle dE/dx \rangle$  versus rigidity measured by TPC in 2014 Au+Au collisions at  $\sqrt{s_{NN}}=200$  GeV



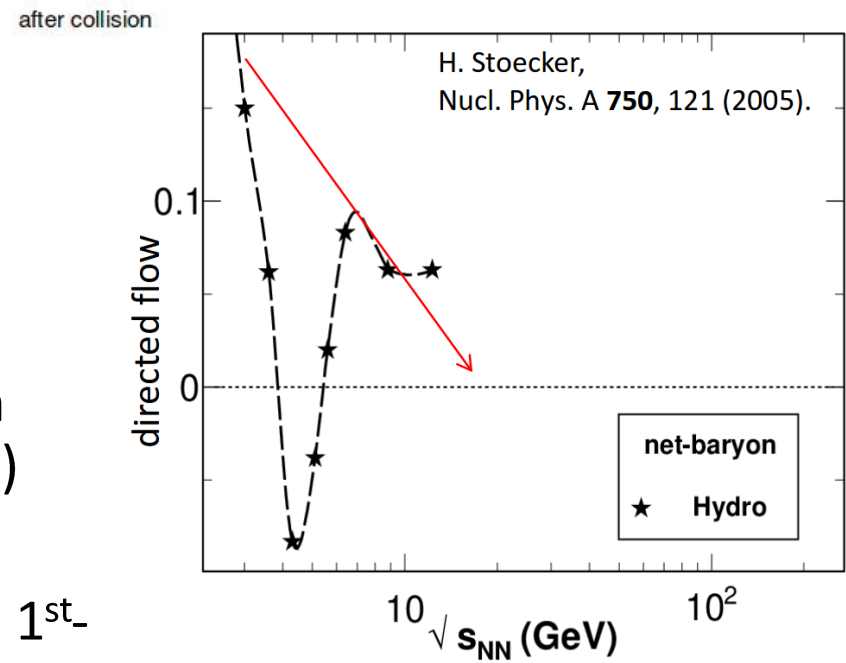
- The  $1/\beta$  versus rigidity measured by TOF in 2014 Au+Au collisions at  $\sqrt{s_{NN}}=200$  GeV



$$E \frac{d^3 N}{d^3 p} = \frac{1}{2\pi} \frac{d^2 N}{p_t dp_t dy} \left( 1 + \sum_{n=1}^{\infty} 2v_n \cos[n(\phi - \Psi_r)] \right)$$

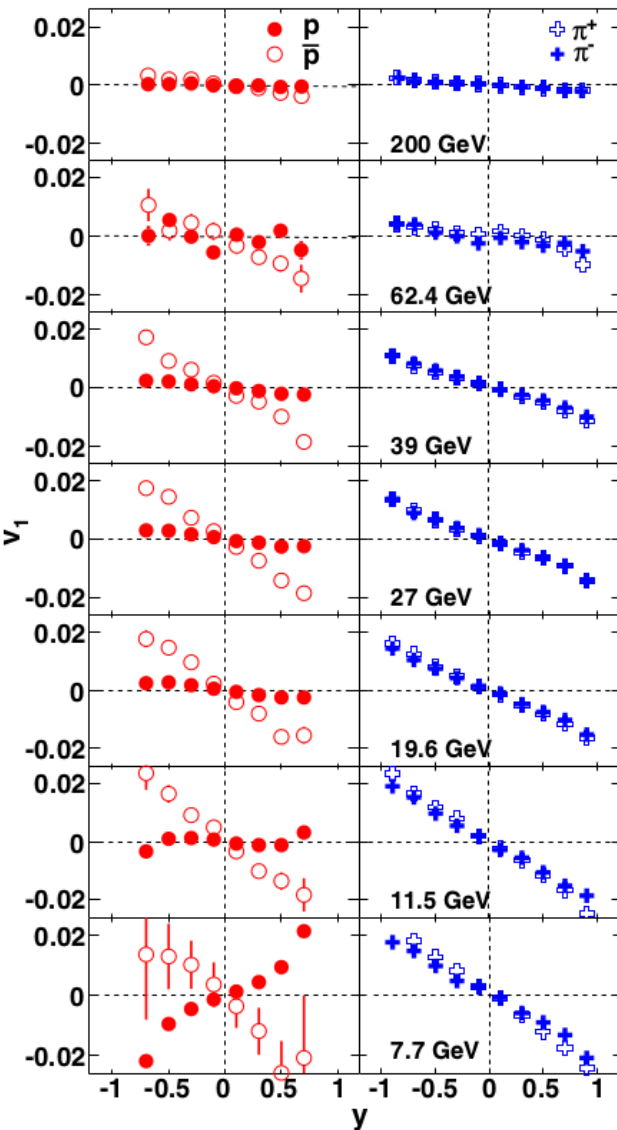
Voloshin, Zhang. *Z. Phys. C* 70 (1996) 665  
 Poskanzer, Voloshin. *Phys. Rev. C* 58 (1998) 1671

- $v_1 = \langle p_x / p_t \rangle$  – directed flow
- Describes the sideward collective motion of particles within the reaction plane (x-z)
- Probe of the softening of the EoS:
  - Strong softening: consistent with the 1<sup>st</sup>-order phase transition
  - Weaker softening: more likely due to crossover



Nara, Niemi, Steinheimer, Stöcker. *Phys. Lett. B* 769 (2017) 543  
 Ivanov, Soldatov. *Phys. Rev. C* 91 (2015) 024915

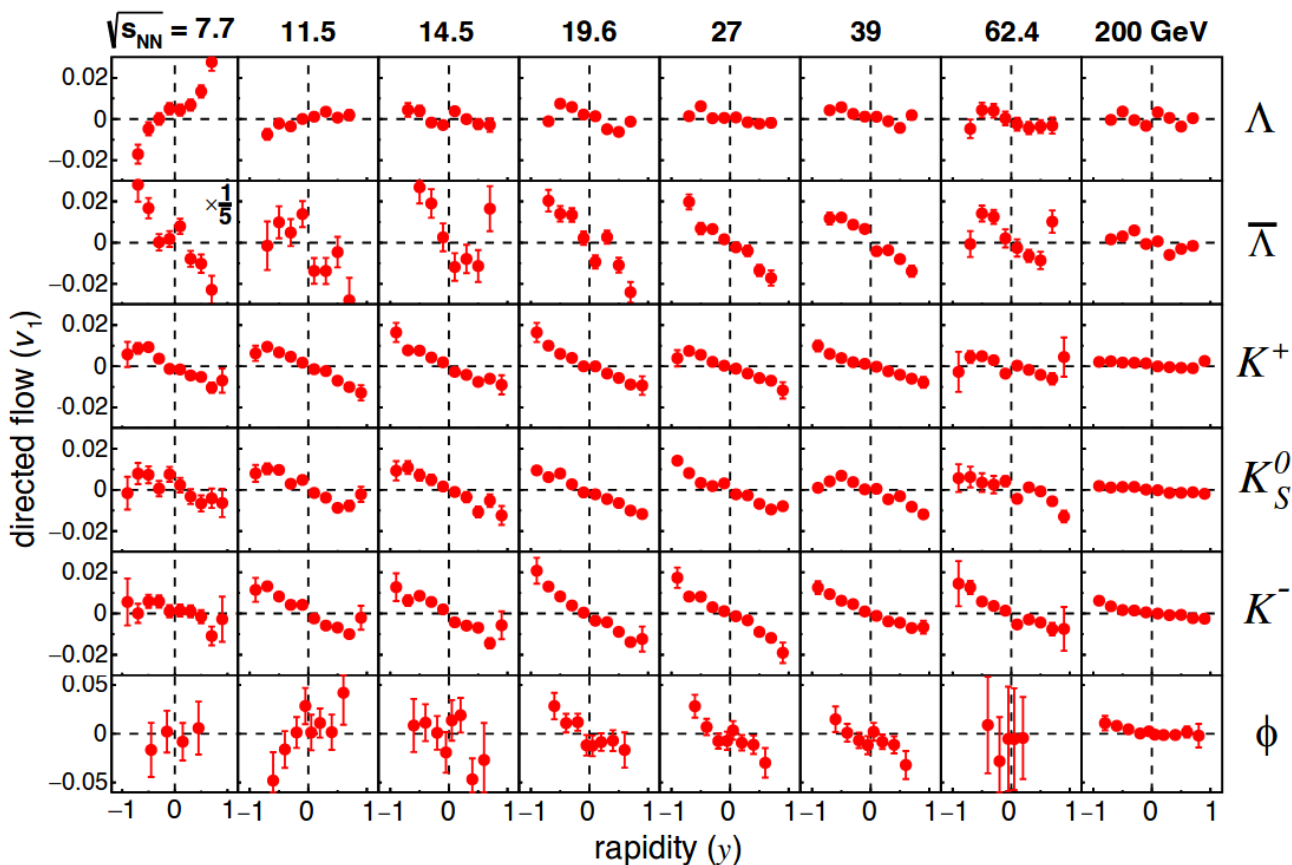
10-40% Au+Au collisions

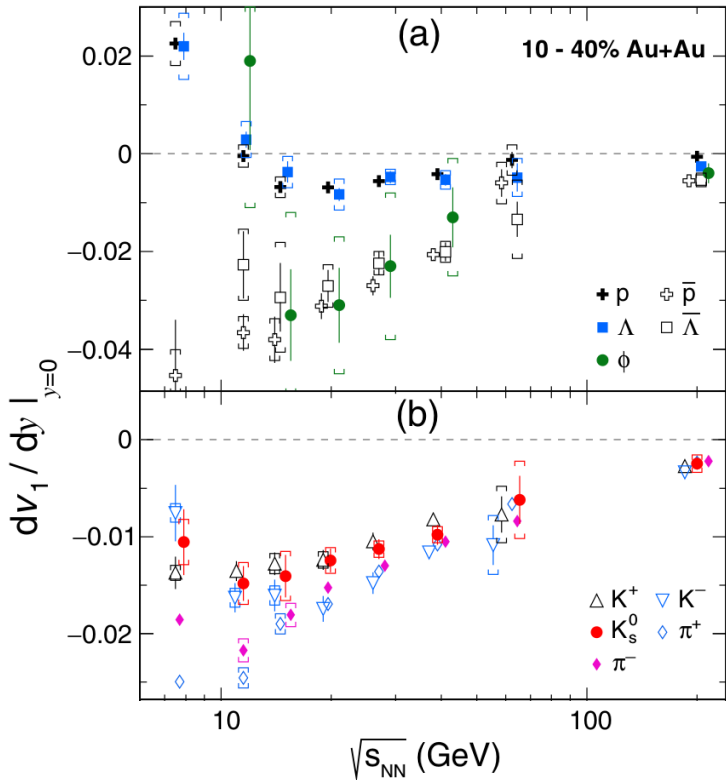


To extract  $v_1$  slope, linear fit was used over  $|y| < 0.6$  for  $\phi$  meson and over  $|y| < 0.8$  for all other species

STAR. Phys. Rev. Lett. 112 (2014) 162301

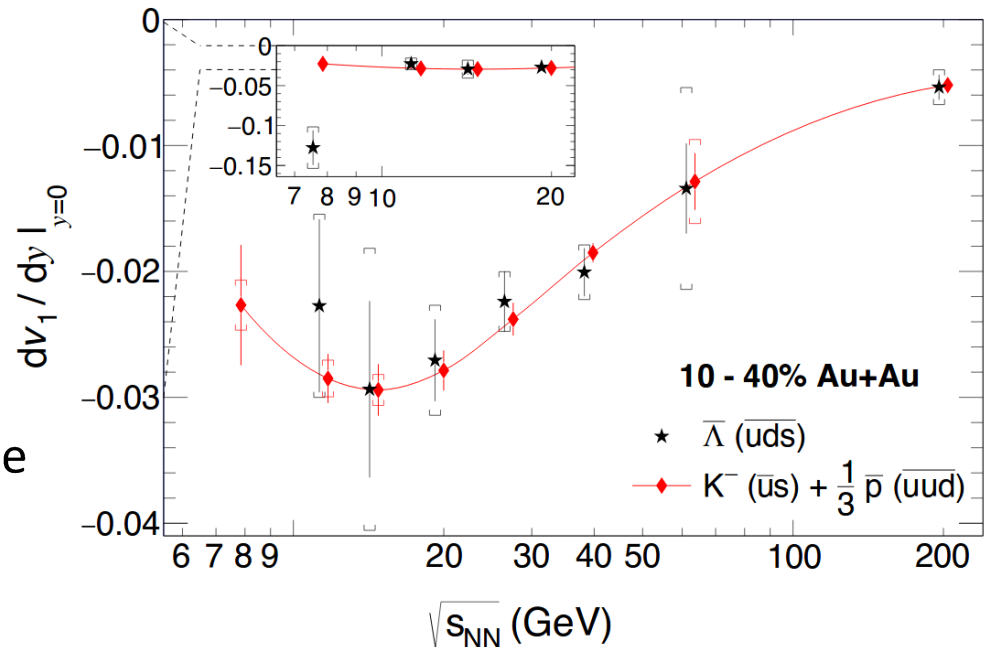
STAR. Phys. Rev. Lett. 120 (2018) 062301





- $dv_1/dy$  for  $\Lambda$  and p agree within uncertainties
- $dv_1/dy$  slope for baryons changes sign in the region  $\sqrt{s_{NN}} < 14.5$  GeV
- Particles (anti-p, anti- $\Lambda$ , and  $\phi$ ) with produced quarks show similar behavior for  $\sqrt{s_{NN}} > 14.5$  GeV
- Mesons show negative  $dv_1/dy$

STAR. Phys. Rev. Lett. 120 (2018) 062301

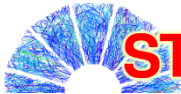


Assumptions for coalescence sum rule:

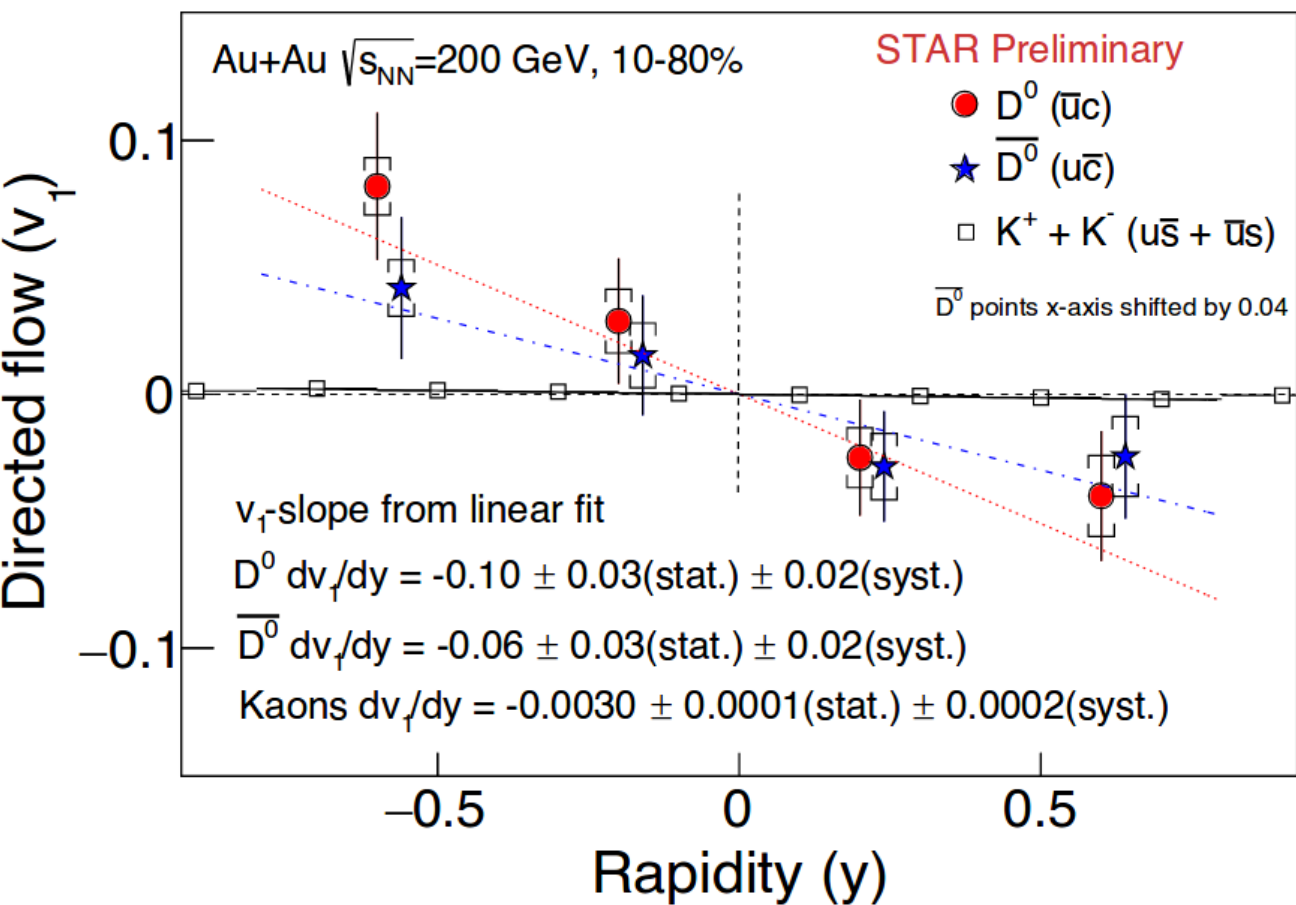
- $v_1$  is developed at prehadronic stage
- Specific types of quarks have the same  $v_1$
- Hadrons are formed via coalescence  
 $(v_n)_{hadron} = \sum (v_n)_{constituent\ quarks}$

For anti-Lambdas, prediction using coalescence sum rule agrees with measured  $v_1$  above  $\sqrt{s_{NN}}=11.5$  GeV

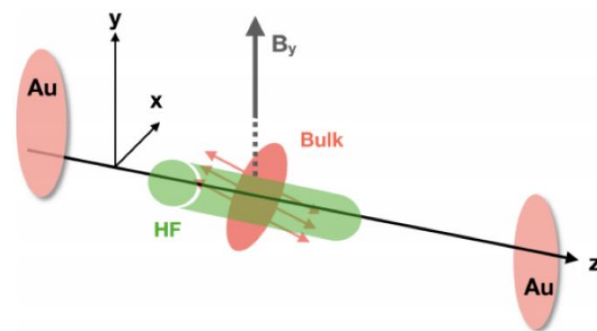




# STAR ☆ $v_1$ of $D^0$ in Au+Au at 200 GeV



Interplay between the drag by the tilted bulk and the EM field



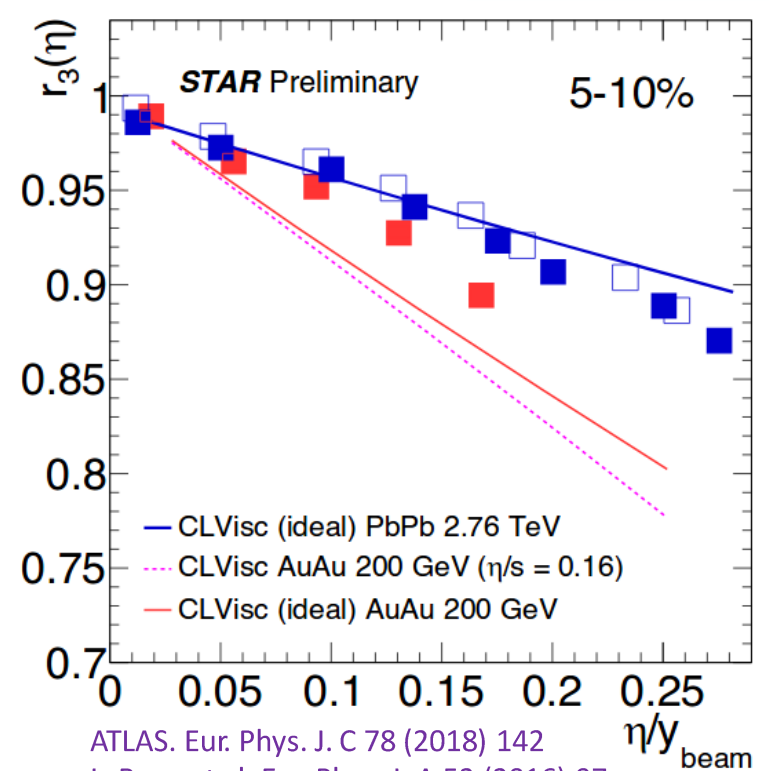
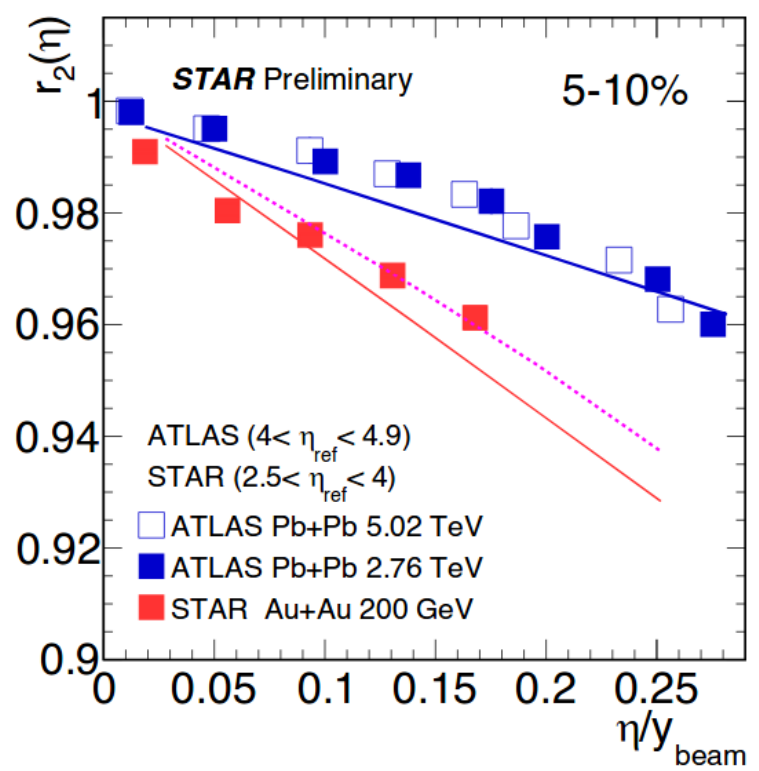
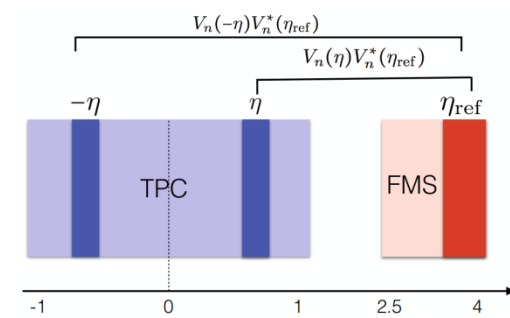
Chatterjee, Bozek. Phys. Rev. Lett. 120 (2018) 192301

First evidence for non-zero  $D^0$   $v_1$  from 2014+2016 Heavy Flavor Tracker (HFT) data:

$$D^0 + \bar{D}^0 \, dv_1/dy = -0.081 \pm 0.021(\text{stat.}) \pm 0.017(\text{syst.})$$

CMS. Phys. Rev. C 92 (2015) 034911

$$r_n(\eta) = \frac{\langle v_n(-\eta)v_n(\eta_{\text{ref}}) \cos n(\Psi_n(-\eta) - \Psi_n(\eta_{\text{ref}})) \rangle}{\langle v_n(\eta)v_n(\eta_{\text{ref}}) \cos n(\Psi_n(\eta) - \Psi_n(\eta_{\text{ref}})) \rangle}$$



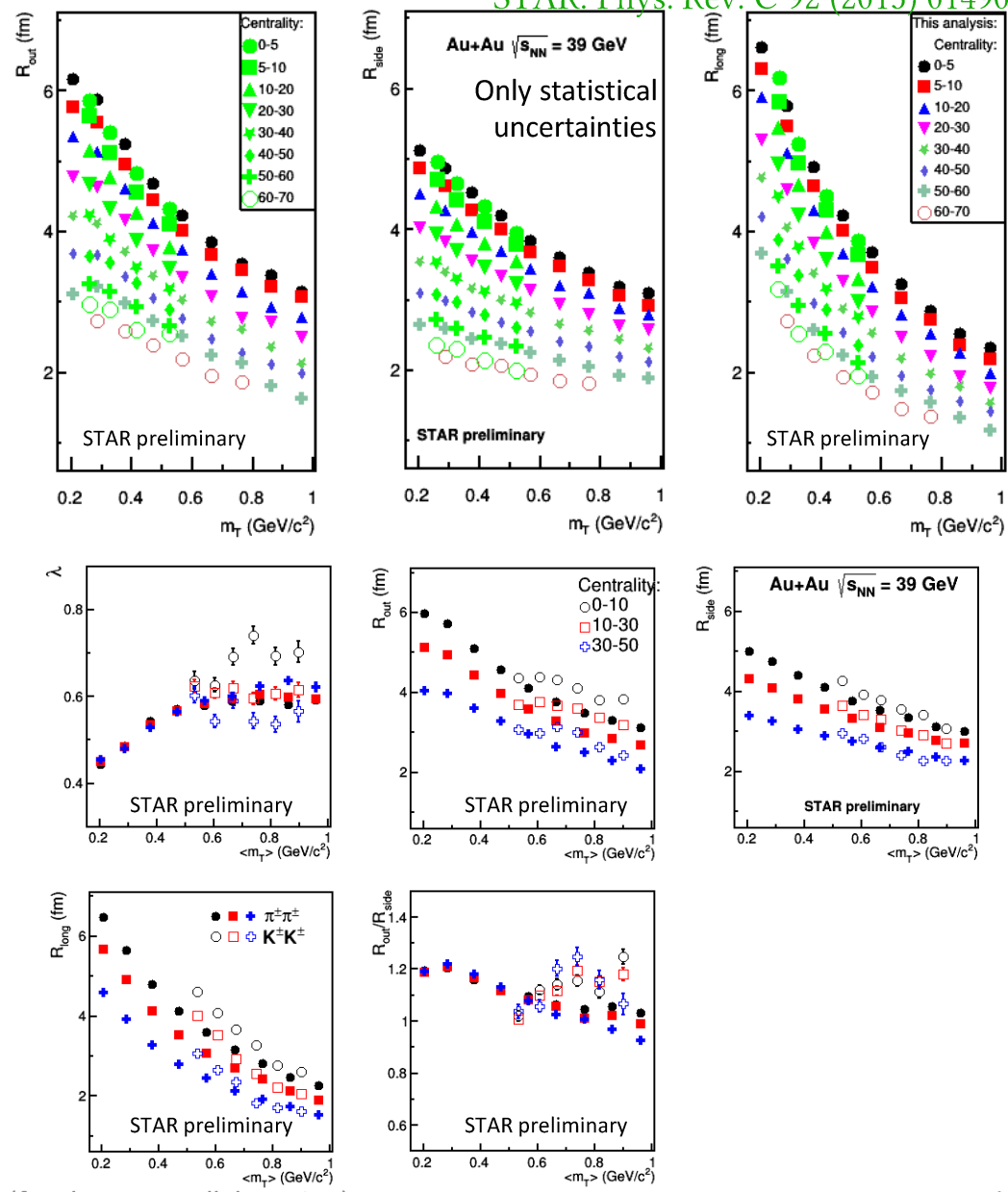
ATLAS. Eur. Phys. J. C 78 (2018) 142  
 L. Pang et al. Eur. Phys. J. A 52 (2016) 97  
 L. Pang et al. arXiv: 1802.04449

- Stronger longitudinal flow decorrelation at RHIC than at LHC
- Hydrodynamic calculations can not simultaneously describe LHC and RHIC data



- Use two-particle momentum correlations to measure spatial and temporal properties of the source at kinetic freeze-out
- Utilizing the information from the TOF detector to extend measurement to higher transverse mass ( $m_T$ ) region

- Kaon femtoscopic radii in outward and longitudinal directions are generally larger than those for pions at the same  $m_T \rightarrow$  breaking of the  $m_T$ -scaling
- In the sideward direction, the pion and kaon radii are similar

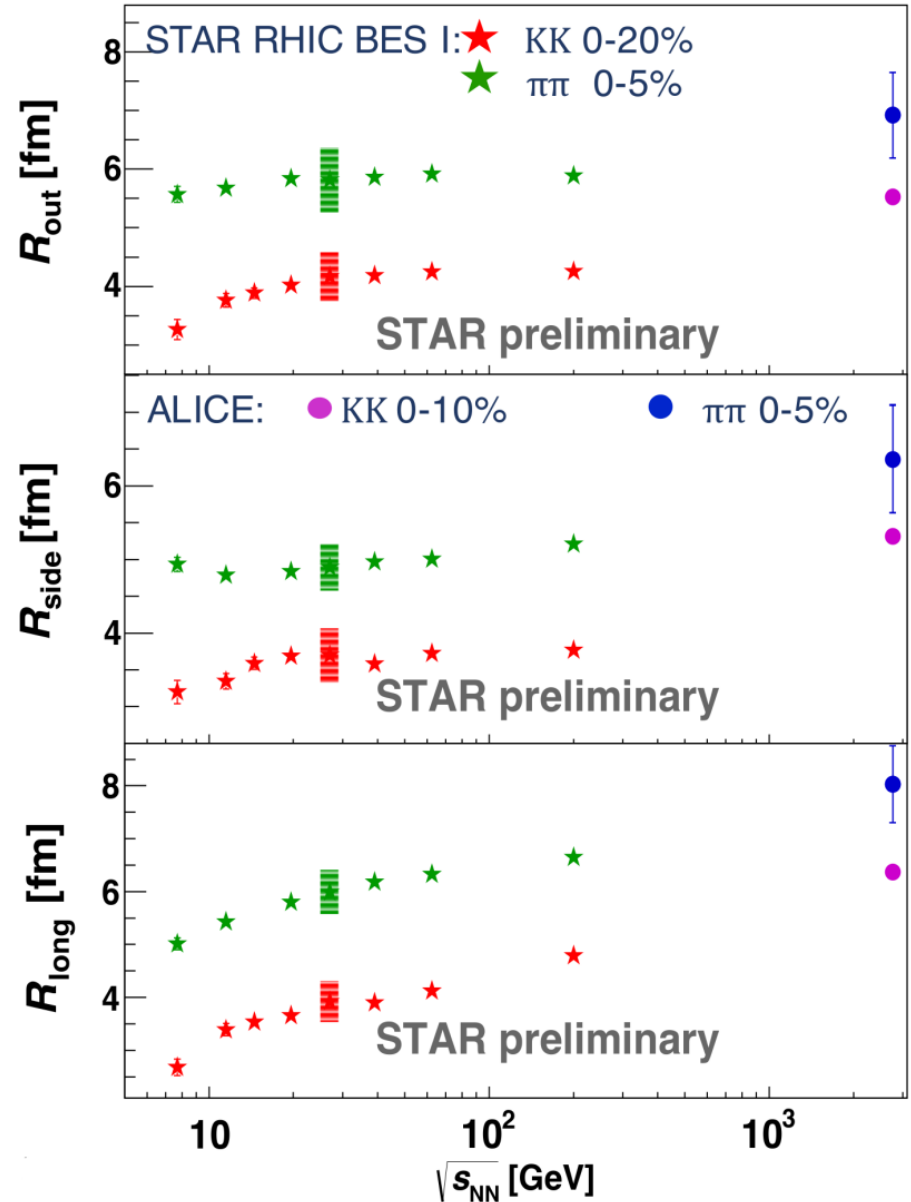


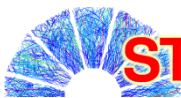


The extracted femtoscopic radii smoothly increase with increasing collision energy

The values of  $R_{out}$  and  $R_{side}$  for both pions and kaons show a very small increase at the RHIC energies and slightly larger at the LHC

The values of  $R_{long}$  suggest that the system lives longer at the LHC energy





## Diffraction in $\rho^0$ photoproduction

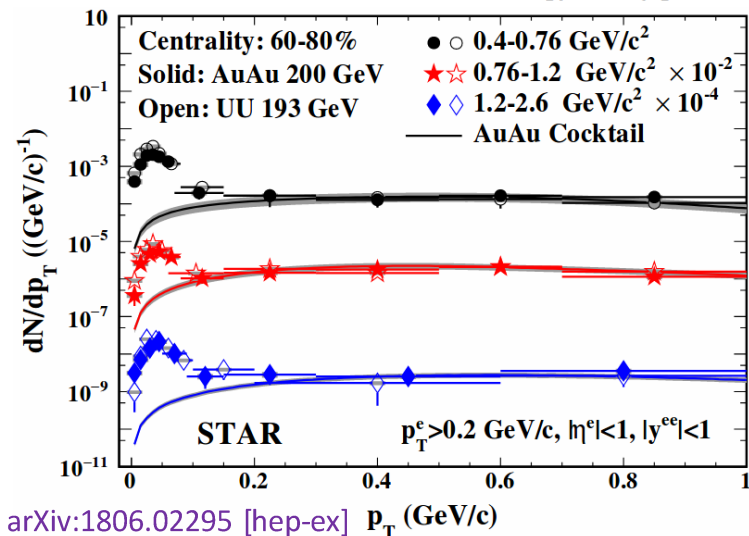
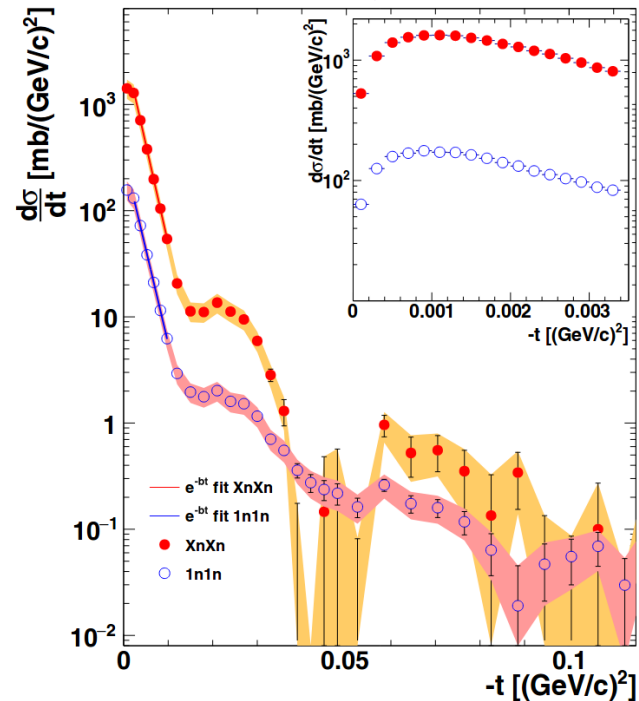
- $-t$  is the square of transferred 4-momentum
- Diffractive dips at  $-t=0.018$  and  $0.043$  (GeV/c)<sup>2</sup>
- Two cases of nuclear breakup:
  - 1n1n: one neutron at (+) and (-) rapidity
  - XnXn: one or more neutrons at (+) and (-) rapidity
- Exponential slope in  $d\sigma/dt$  is consistent with LHC (ALICE. JHEP 1509 (2015) 095)

**Similarity in exponential parts implies no evidence for increase of nuclear size with photon energy**

## Electromagnetic processes in peripheral collisions

- Data on  $e^+e^-$  pairs in peripheral Au+Au and U+U collisions
- Yield enhanced at low  $p_T$  with respect to hadronic expectation
- Shape of the excess is consistent with  $e^+e^-$  from photoproduction

**Novel probe to electromagnetic fields of the nuclei**

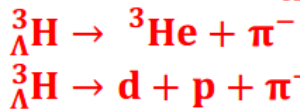


STAR. arXiv:1806.02295 [hep-ex]  $p_T$  (GeV/c)



# (Anti)Hypertriton Binding Energy

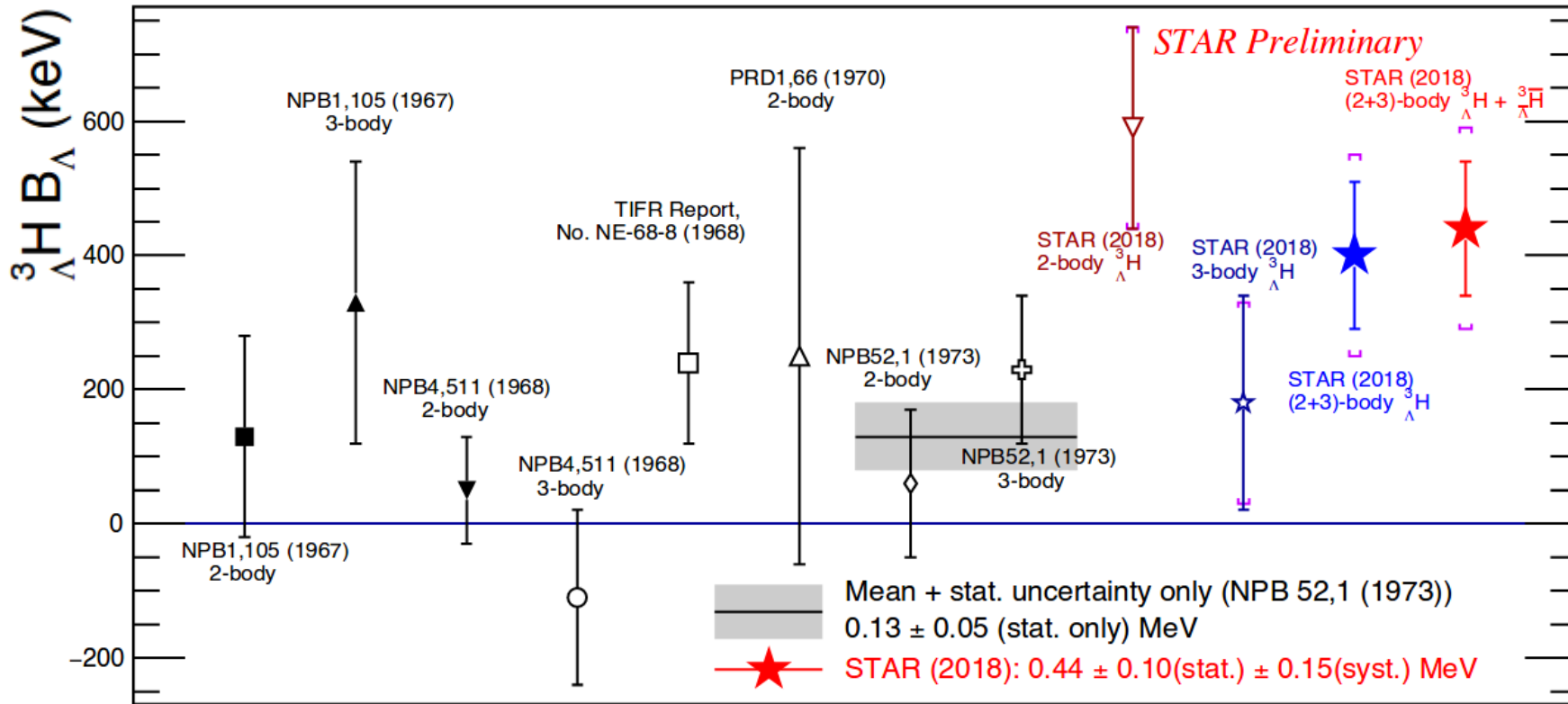
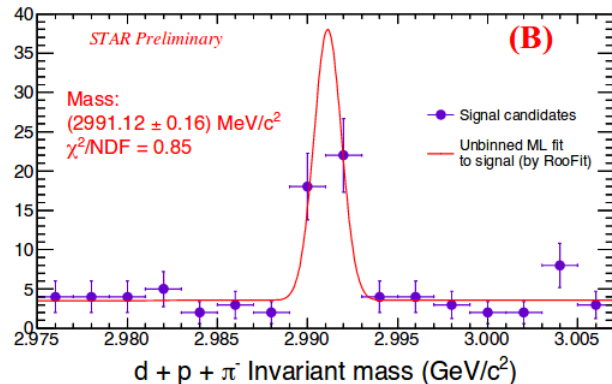
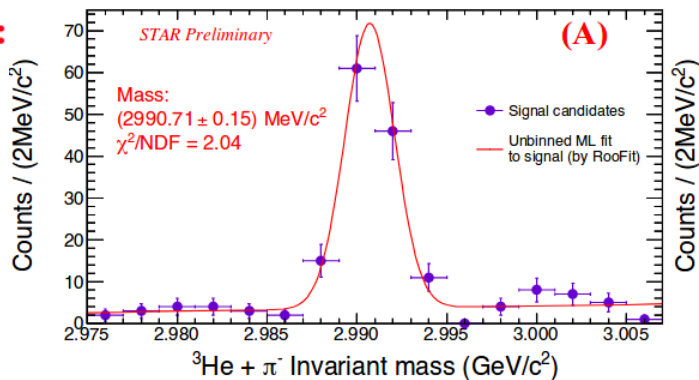
Reconstructing  ${}^3_{\Lambda}\text{H}$  ( ${}^3_{\Lambda}\bar{\text{H}}$ ) through:

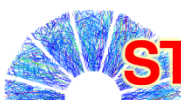


Binding energy ( $B_{\Lambda}$ )

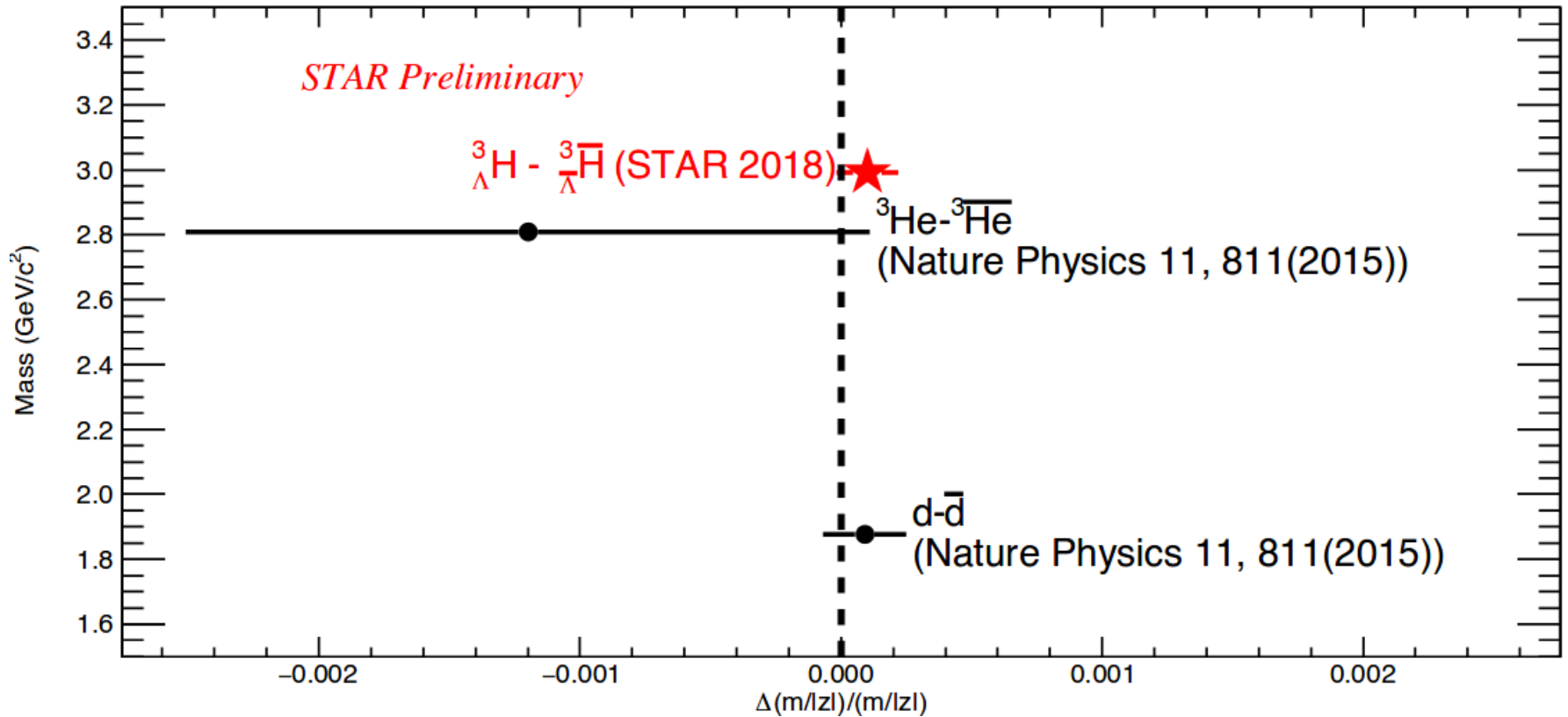
definition:

$$m_{\Lambda} + m_{\text{d}} - m_{{}^3_{\Lambda}\text{H}}$$





# Mass difference between ${}^3_{\Lambda}H$ and ${}^3_{\Lambda}\bar{H}$



- First measurement of the hypertriton and antihypertriton mass difference

- Test of CPT symmetry in the light hypernuclei sector

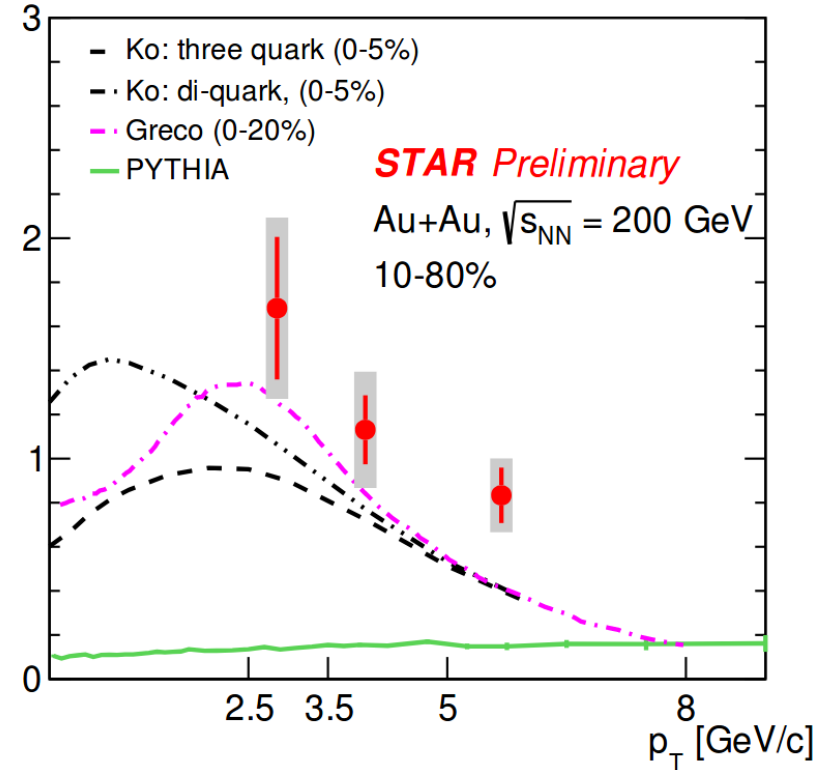
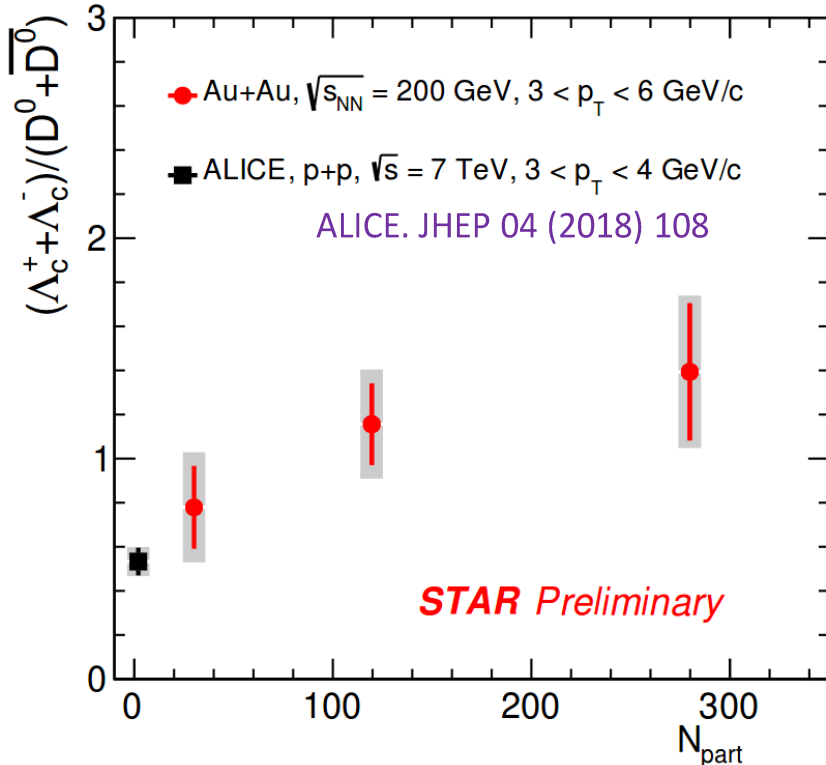
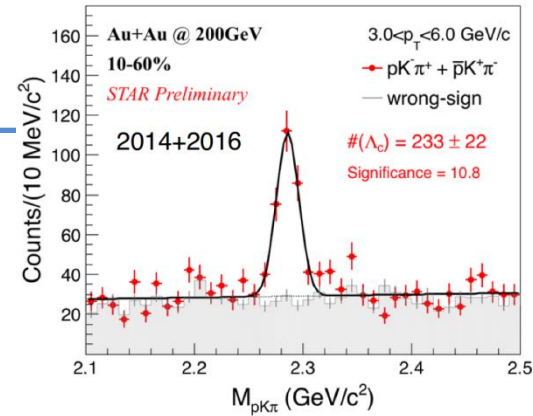
$$\left(\frac{\Delta(m/|z|)}{m/|z|}\right)_d = (0.9 \pm 0.5 \text{ (stat.)} \pm 1.4 \text{ (syst.)}) \times 10^{-4}$$

$$\left(\frac{\Delta(m/|z|)}{m/|z|}\right)_{{}^3\text{He}} = (-1.2 \pm 0.9 \text{ (stat.)} \pm 1.0 \text{ (syst.)}) \times 10^{-3}$$

$$\left(\frac{\Delta m}{m}\right)_{{}^3_{\Lambda}\text{H}} = (1.0 \pm 0.9 \text{ (stat.)} \pm 0.7 \text{ (syst.)}) \times 10^{-4}$$

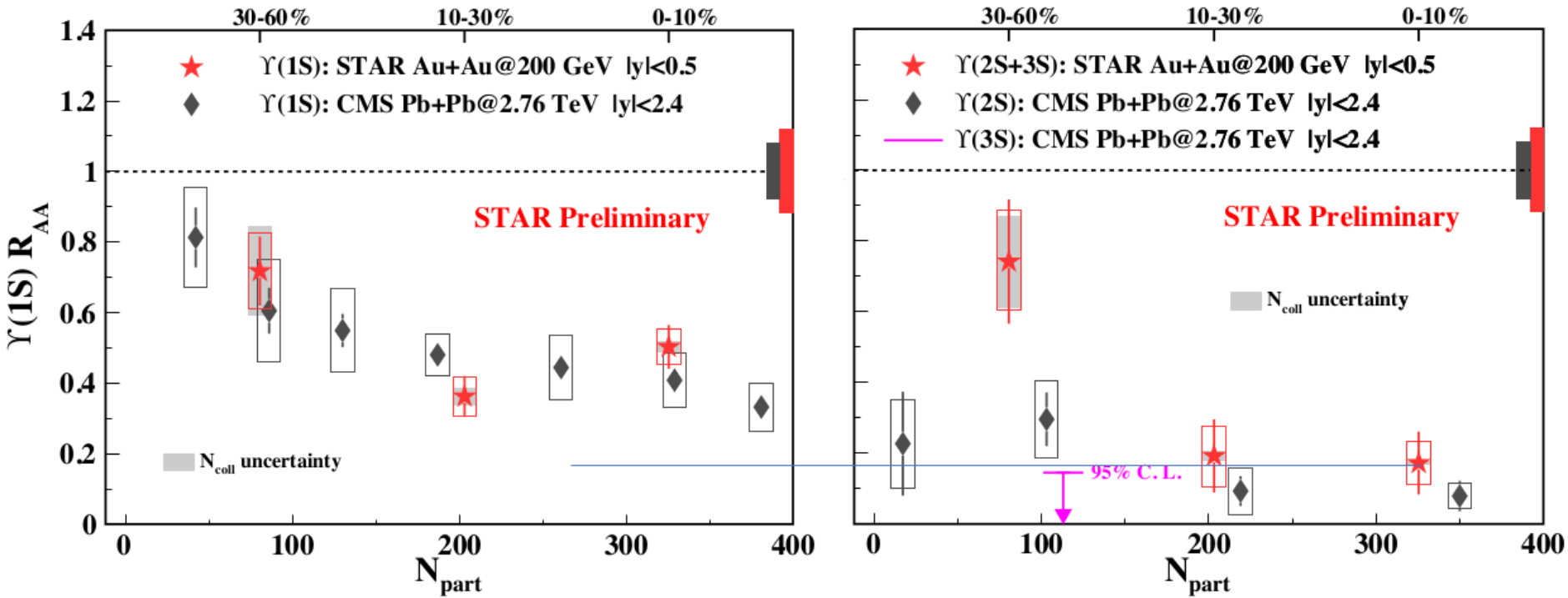
- The mass difference is consistent with the CPT expectation

Adding data from year 2016 and using TMVA BDT allowed to obtain more than 2 times improvement in the signal significance than 2014 data alone



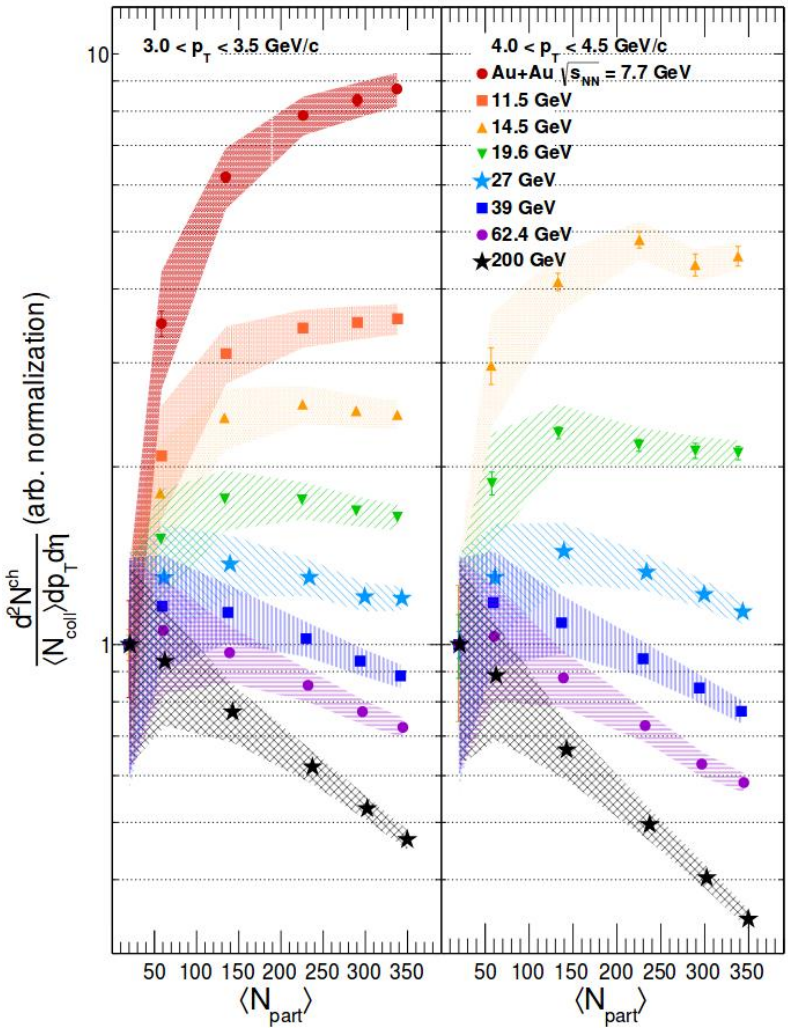
- $\Lambda_c/D^0$  ratio increases from peripheral to central collisions
- Enhancement of  $\Lambda_c$  production increases towards low  $p_T$
- Large  $\Lambda_c$  contribution to the total charm cross-section in heavy-ion collisions





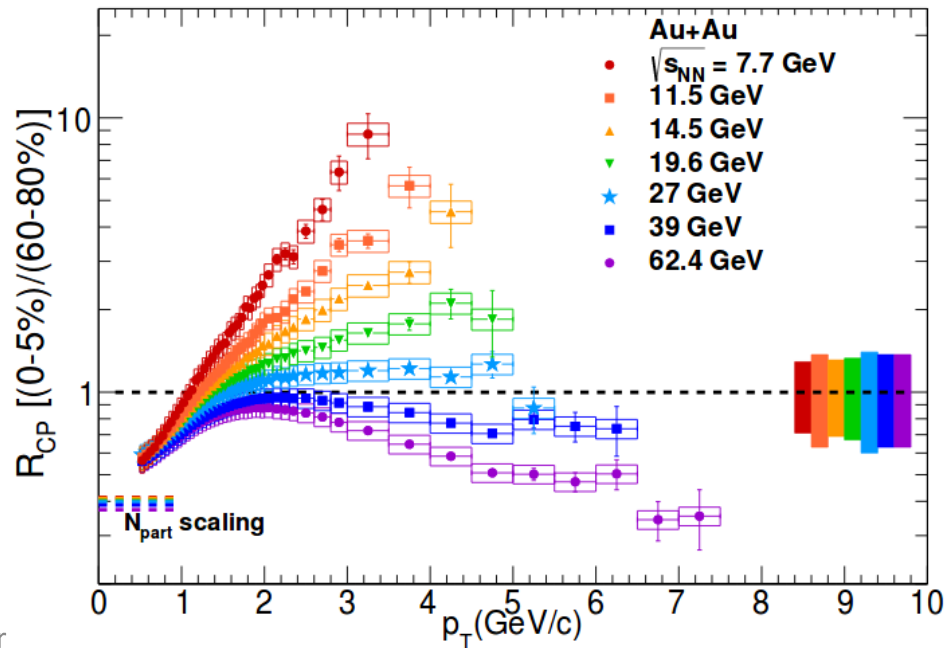
CMS. Phys. Lett. B 04 (2017) 031

- Improved precision by combining 2011 di-electron, 2014+2016 di-muon
- $Y(2S+3S) R_{AA}$  smaller than  $Y(1S)$  in 0-10%
  - “Sequential melting” at RHIC



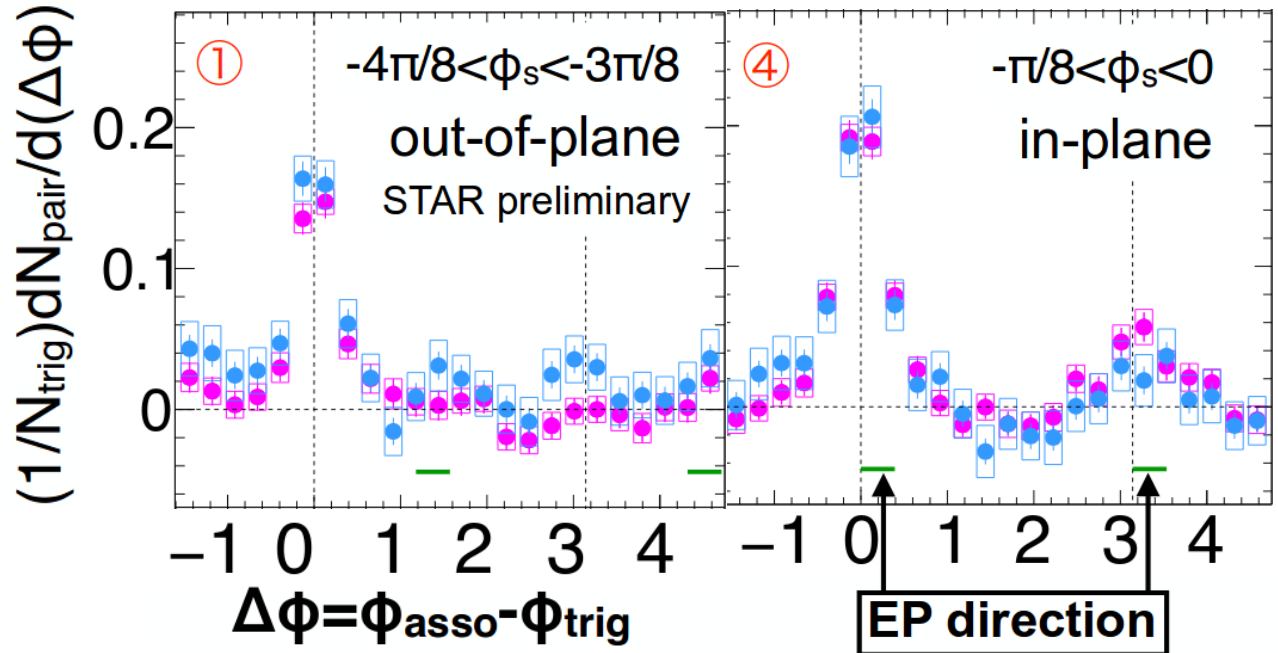
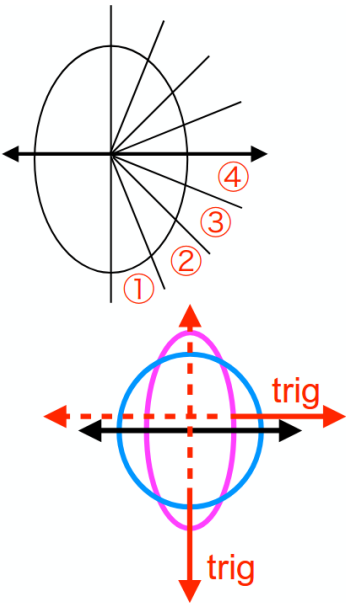
STAR. arXiv: 1707.01988v1

- $R_{CP}$  for hadrons and for charged particles probes partonic energy loss in the medium
- BES-I results Indicate disappearance of suppression below 14.5 GeV
- Would like to explore this with identified hadrons (to isolate baryon stopping)

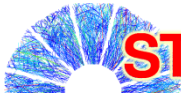




Au+Au  $\sqrt{s_{NN}} = 200$  GeV  
 0-10%  
 ●  $q_2$  top 20%  
 ●  $q_2$  bottom 20%

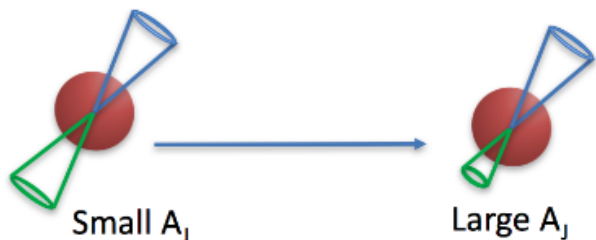


- High- $p_T$  particles penetrate more with short pathlength
- Low- $p_T$  particles are pushed toward in-plane direction and this effect is stronger in large  $q_2$ 
  - Pathlength-dependent jet-medium interaction



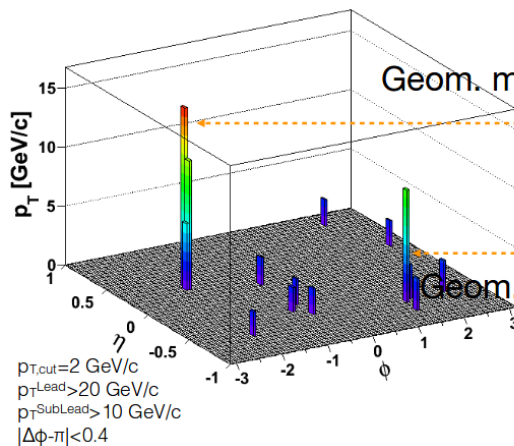
# STAR ☆ “Hard Core” Di-Jets

$$A_J = \frac{p_T^{\text{Lead}} - p_T^{\text{SubLead}}}{p_T^{\text{Lead}} + p_T^{\text{SubLead}}}$$

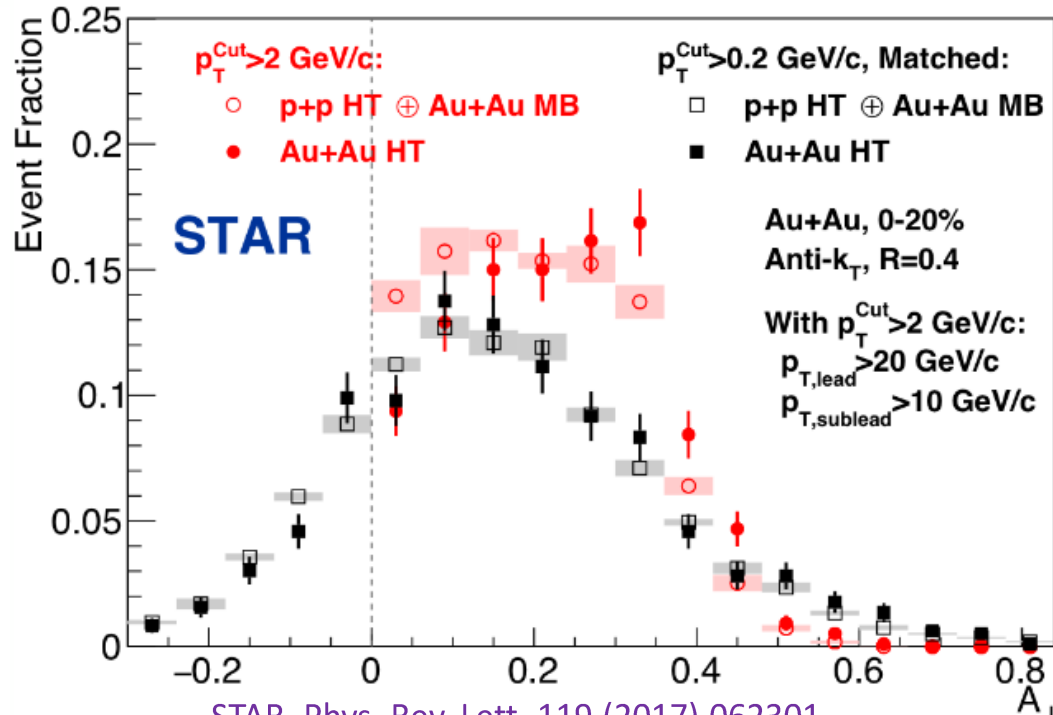
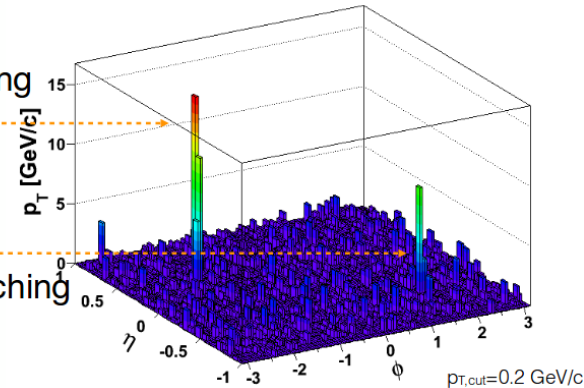


Momentum balance restored to p+p baseline for R=0.4, after adding particles with  $p < 2$  GeV/c

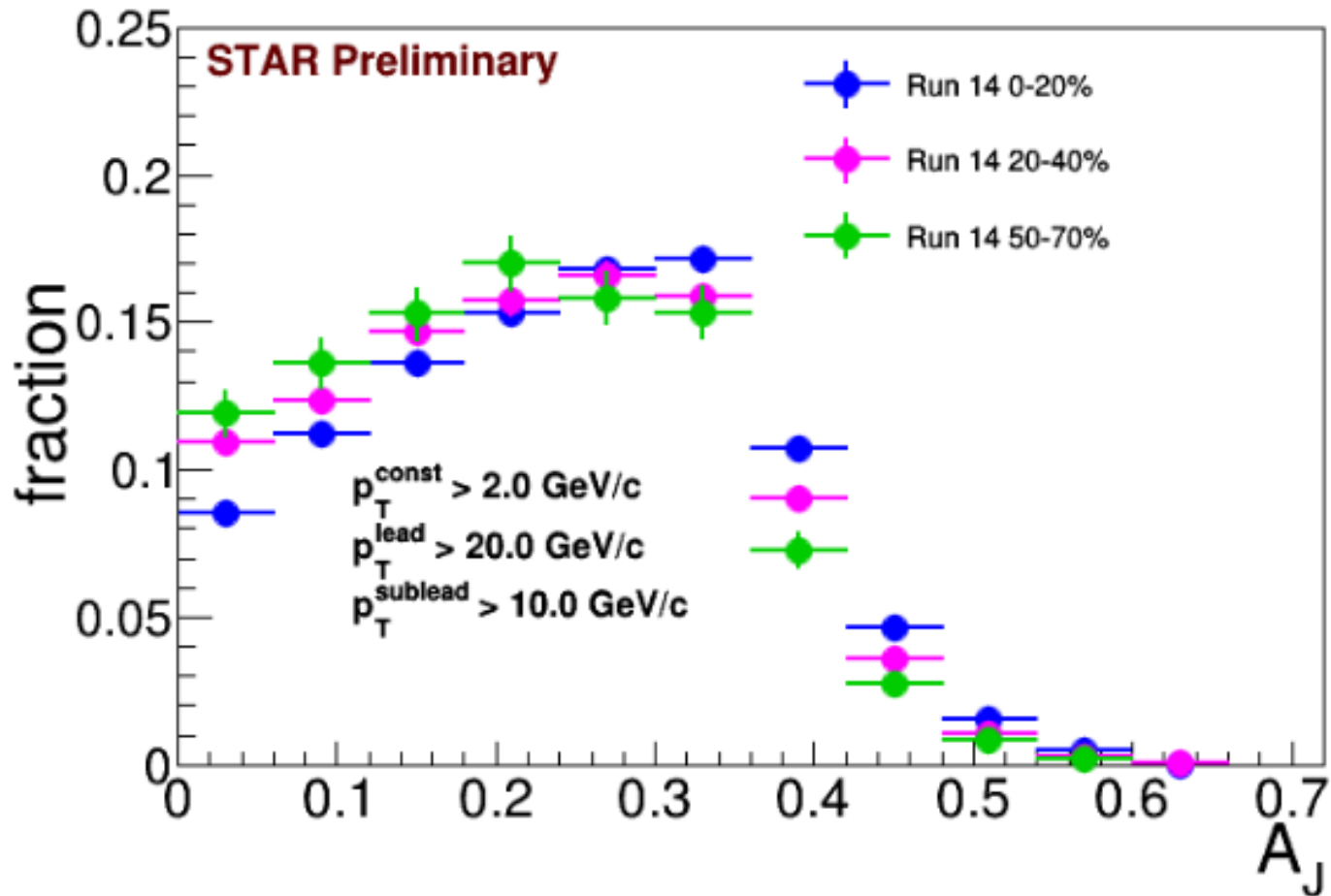
Au+Au w/o soft particles



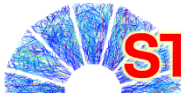
Au+Au w/soft particles



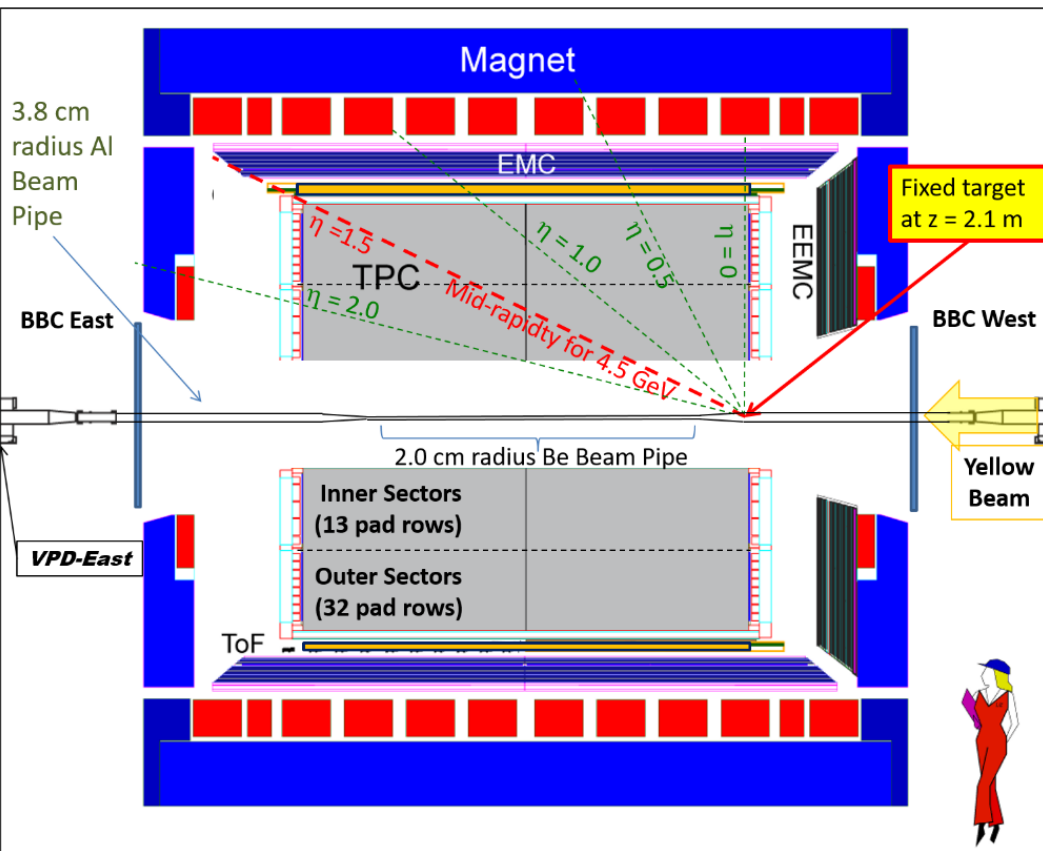
STAR. Phys. Rev. Lett. 119 (2017) 062301



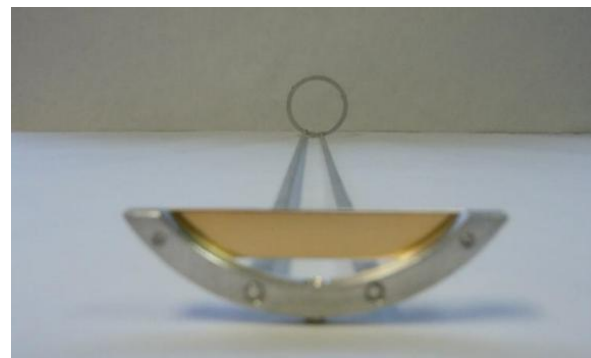
- The first measurement of centrality dependence of  $A_J$  at RHIC
- Smaller di-jet imbalance in more peripheral collisions



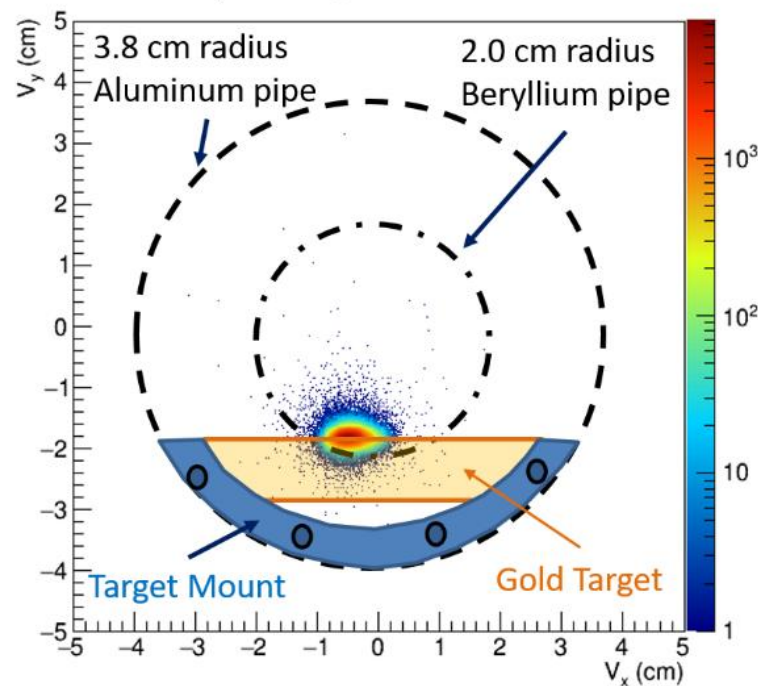
# STAR Fixed-Target Program



A 1 mm thick (4% inter. prob.) gold target

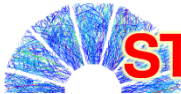


### $V_y$ vs. $V_x$ Distribution



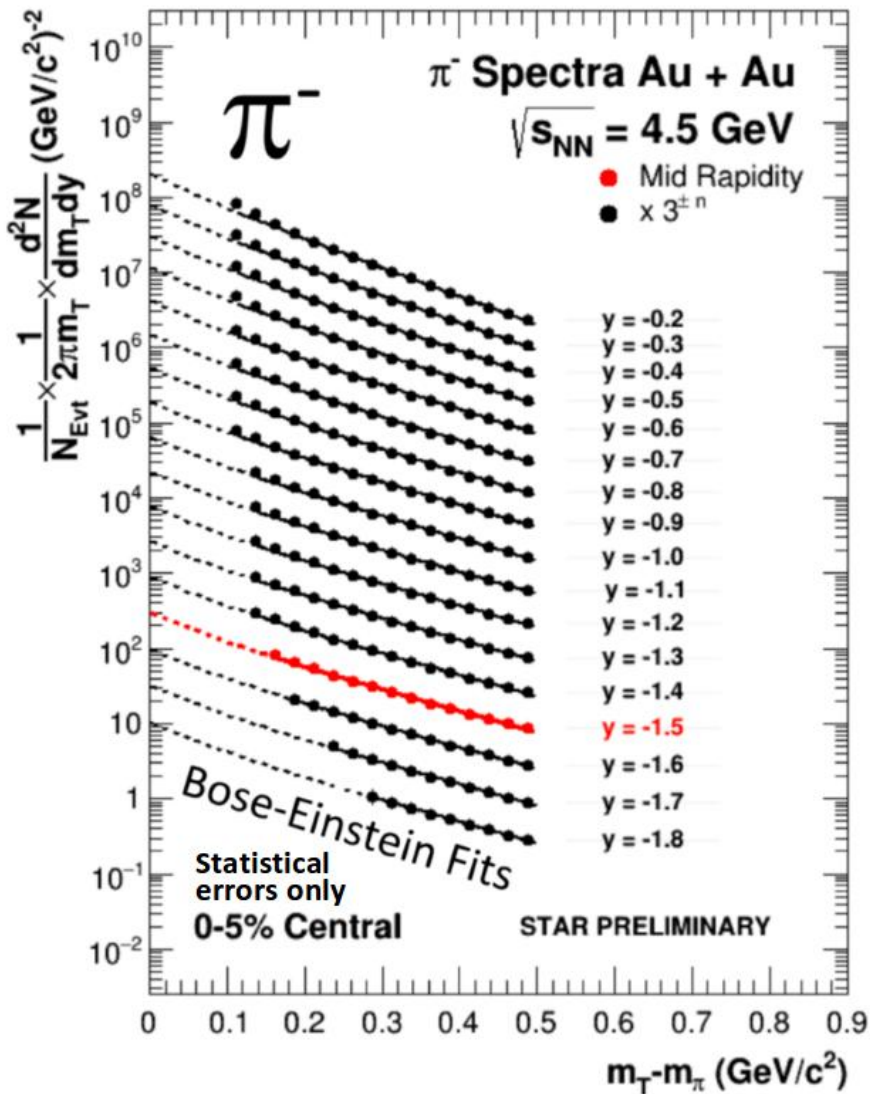
1.3M events from half hour test run, top 30% central trigger, Au+Au  $\sqrt{s_{NN}}=4.5$  GeV

3.4M events from two hour test run, top 30% central trigger, Al+Au  $\sqrt{s_{NN}}=4.9$  GeV

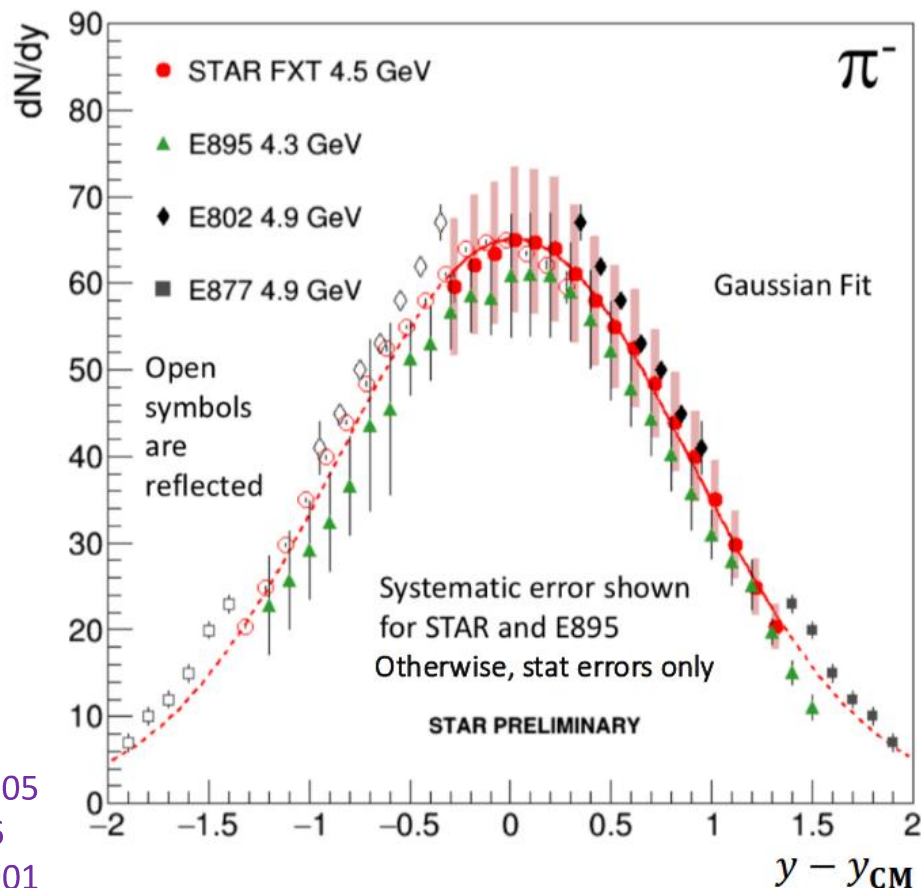


STAR ☆

# Pion spectra and $dN/dy$ in Au+Au at $\sqrt{s_{NN}}=4.5$ GeV



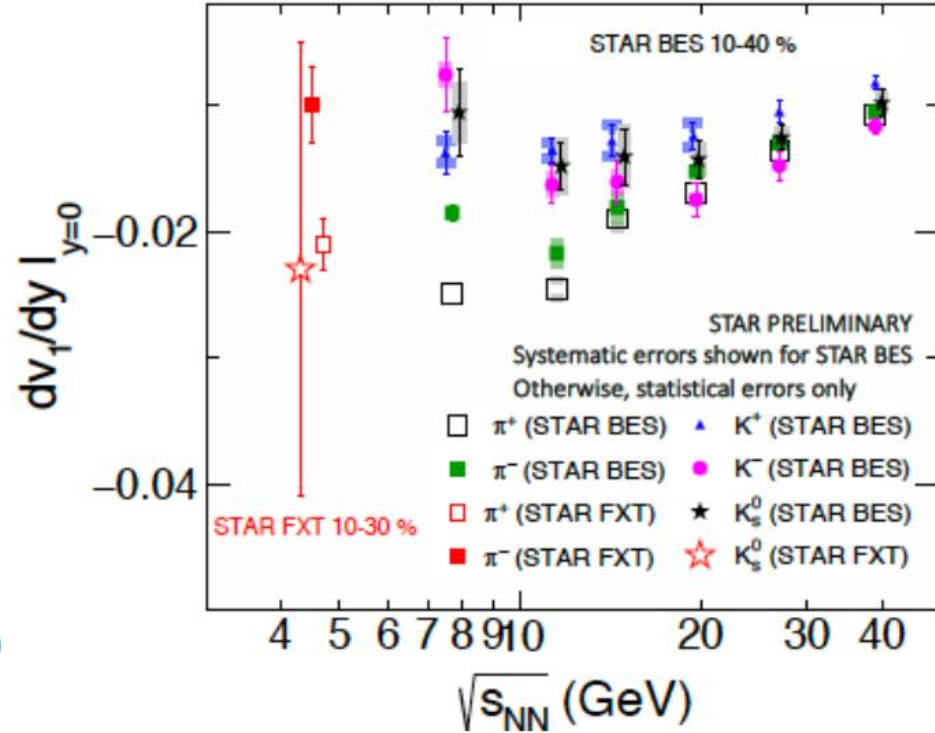
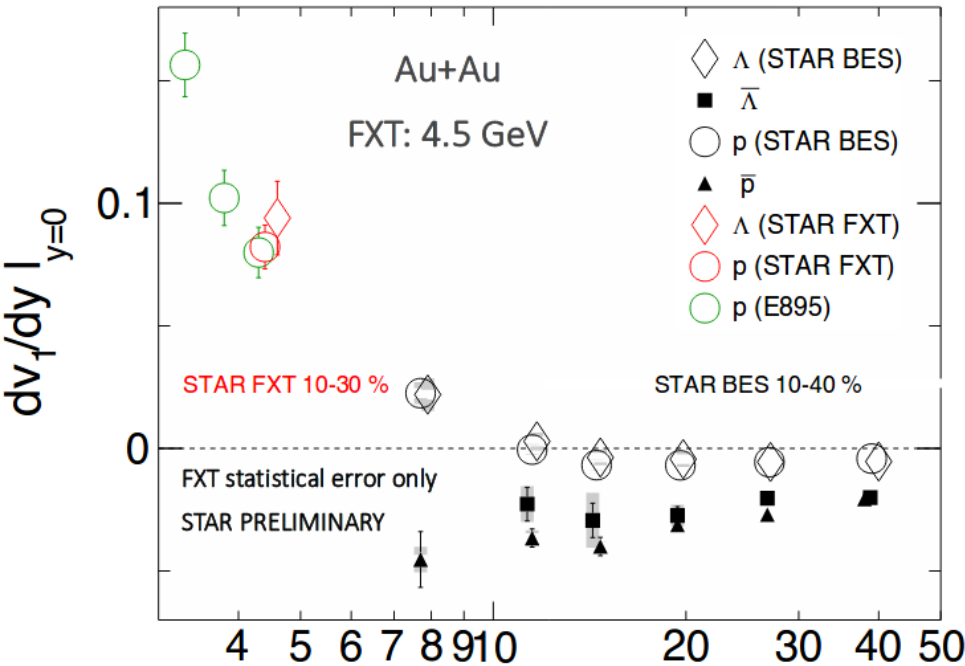
- Amplitudes & widths of rapidity densities are consistent with AGS experiments
- $m_T - m_0$  and  $y$  range will be extended by eTOF & iTPC upgrade



E895. Phys. Rev. C 68 (2003) 054905  
 E802. Phys. Rev. C 57 (1998) R466  
 E877. Phys. Rev. C 62 (2000) 024901



E895. Phys. Rev. Lett. 84 (2000) 005488  
 STAR . Phys. Rev. Lett. 112 (2014) 162301

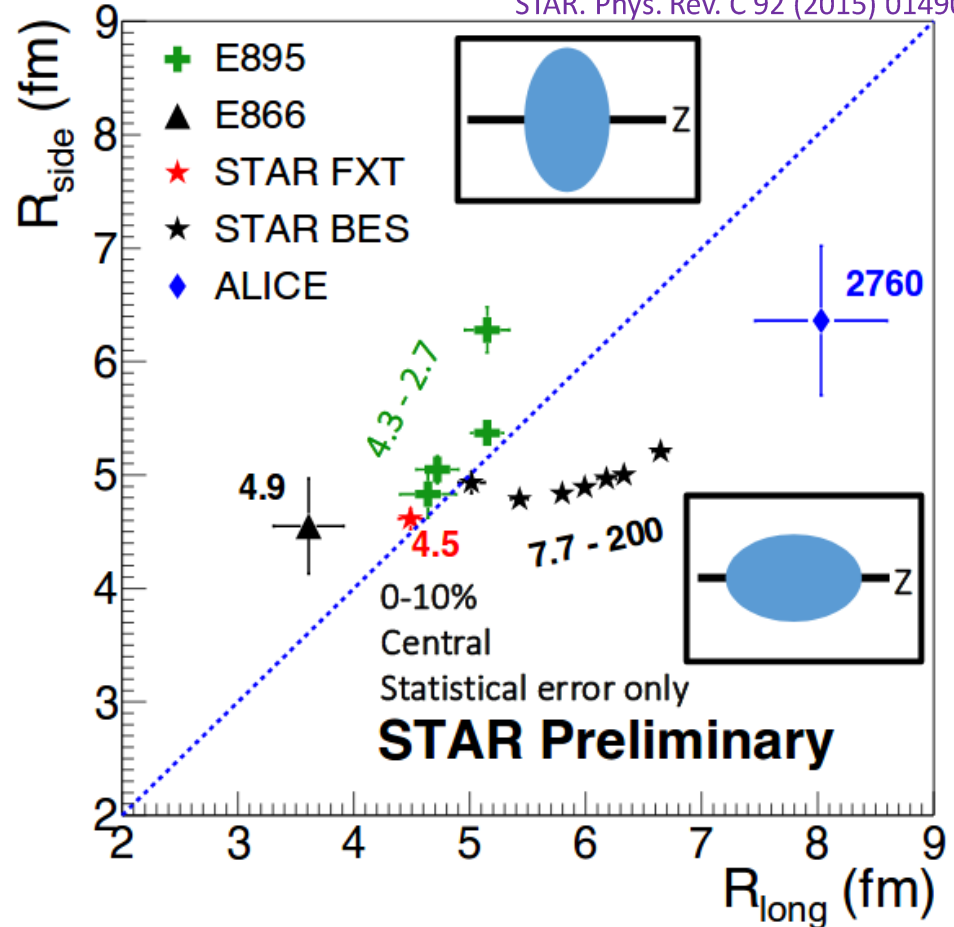
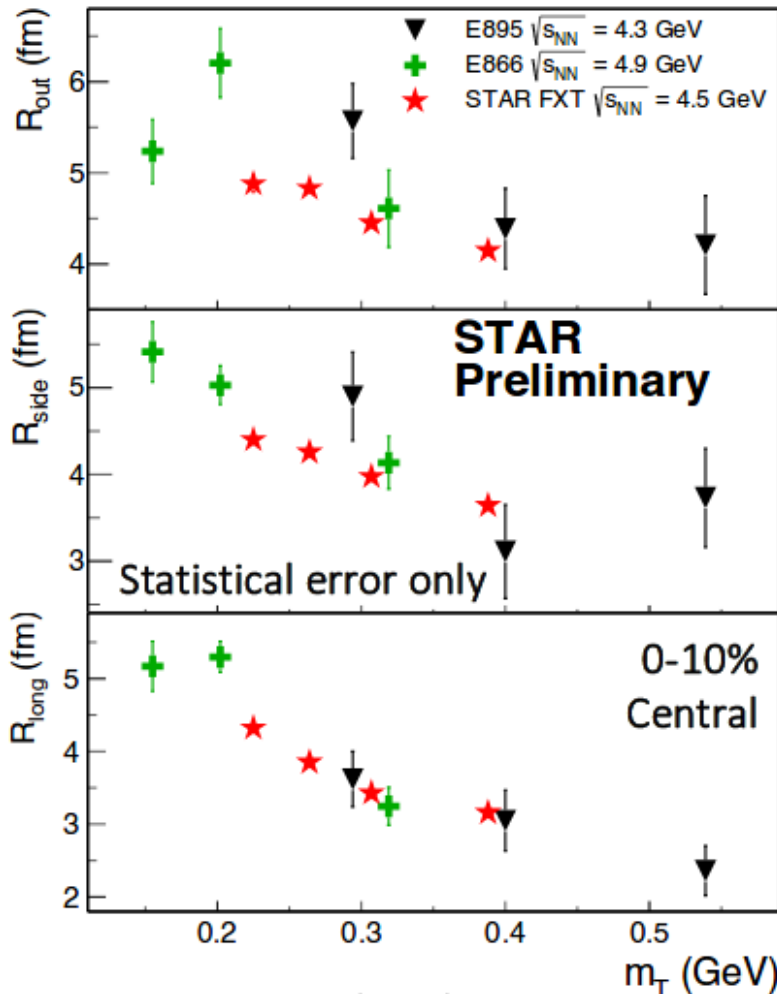


- Proton  $v_1$  is consistent with E895.  $\Lambda v_1$  is close to that of proton
- First pion  $v_1$  measurements in this energy range
- $\pi^+ \pi^-$  ordering supports the idea that transported quarks have bigger effect on  $\pi^-$

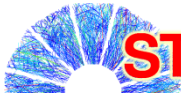




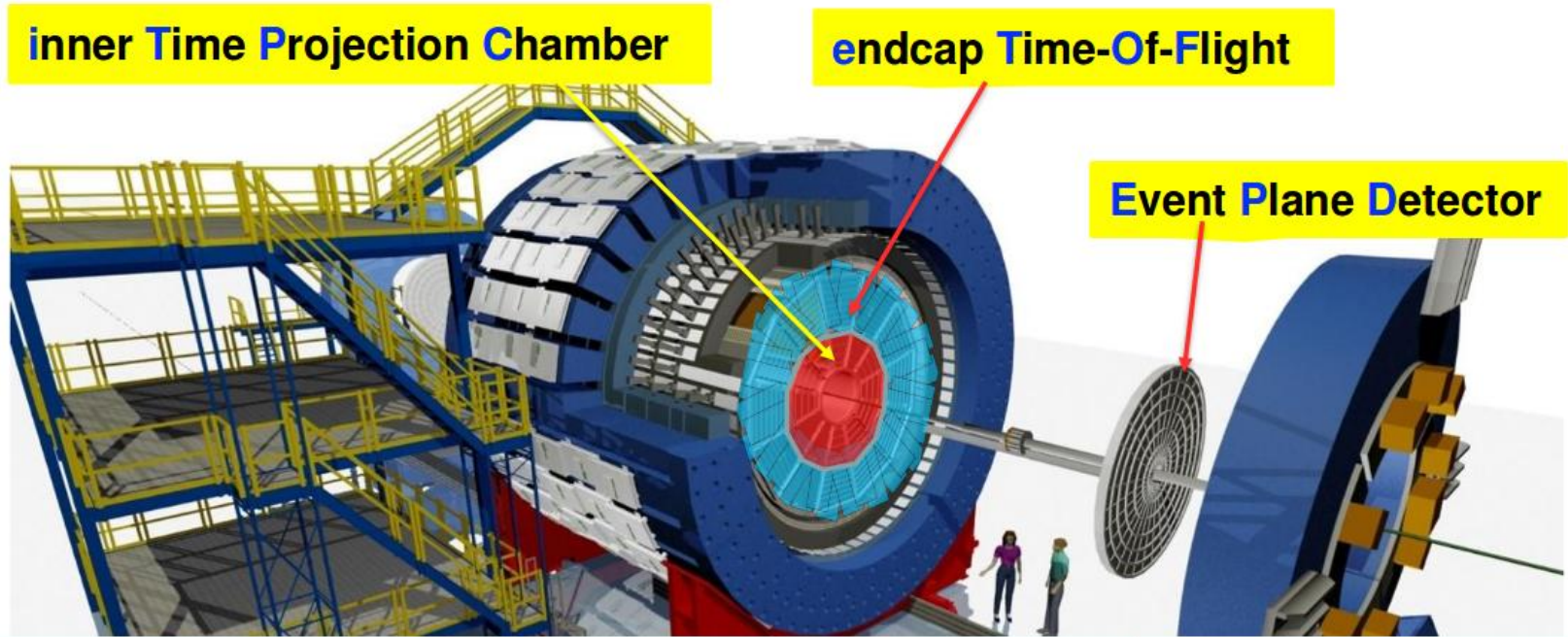
E866. Phys. Rev. C 66 (2002) 054096  
 E895 .Phys. Rev. Lett. 84 (2000) 2798  
 ALICE. Phys. Rev. B 696 (2011) 328  
 STAR. Phys. Rev. C 92 (2015) 014904



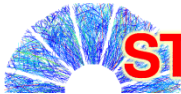
- Consistent with results from AGS experiments, with smaller stat. errors
- Apparent source shape evolves from oblate to prolate, as energy increases
- Increased longitudinal expansion above FXT energy



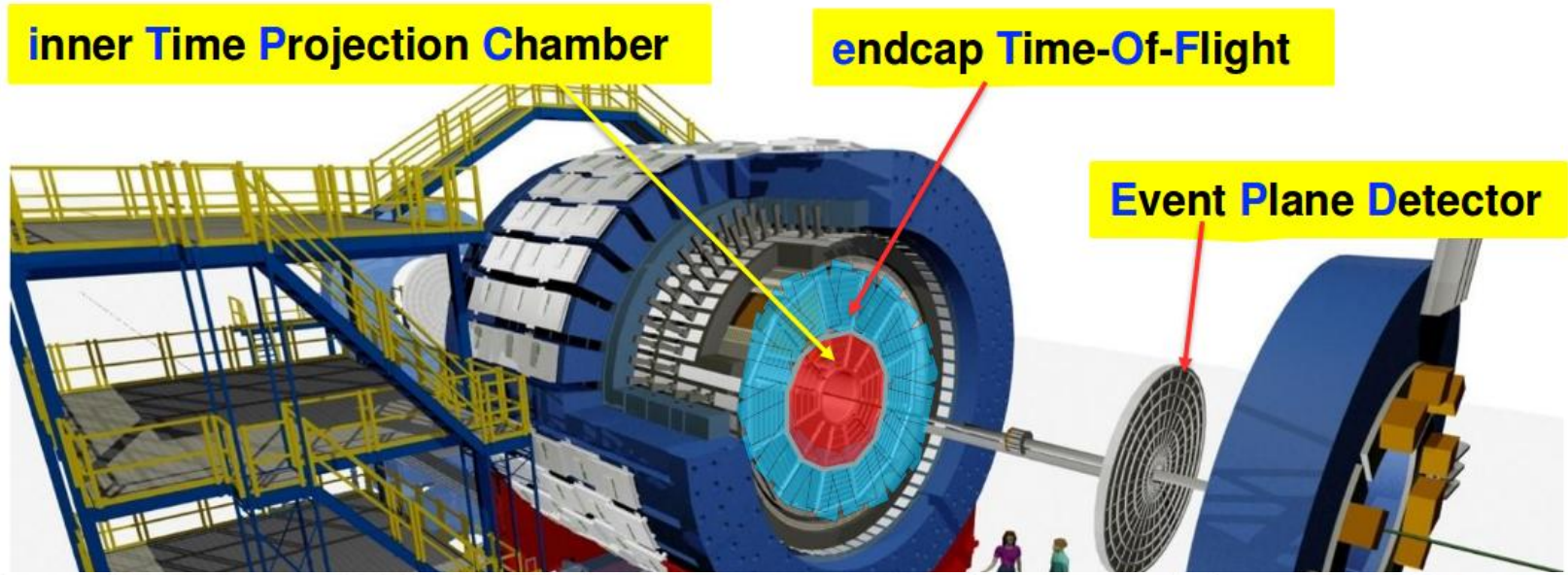
# STAR ☆ Upgrades for BES-II



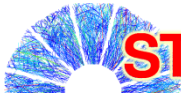
<b>iTPC upgrade</b>	<b>eTOF upgrade</b>	<b>EPD upgrade</b>
Continuous pad rows Replace all inner TPC sectors	Add CBM TOF modules and electronics (FAIR Phase 0)	Replace Beam-Beam Counter
$ \eta  < 1.5$	$-1.6 < \eta < -1.1$	$2.1 <  \eta  < 5.1$
$p_T > 60$ MeV/c	Extend forward PID capability	Better trigger & b/g reduction
Better dE/dx resolution Better momentum resolution	Allows higher energy range of Fixed-Target program	Greatly improved Event Plane info (esp. 1 <sup>st</sup> -order EP)



# STAR ☆ Upgrades for BES-II



- **Inner Sectors**
  - New designed strongback
  - New wire frames
  - Increase readout pad rows (13 to 40)
- **New electronics for inner sectors**
  - Doubled readout channels. Using ALICE SAMPA chip
- **New designed insertion tooling**
  - Removal and insertion of inner sectors
- **Replace all 24 inner sectors**
  - 2018: One sector has been installed and used in the physics run
  - Full installation in autumn 2018



STAR



# The inner TPC upgrade

## • Inner Sectors

- New designed strongback
- New wire frames
- Increase readout pad rows (13 to 40)

## • New electronics for inner sectors

- Doubled readout channels. Using ALICE SAMPA chip

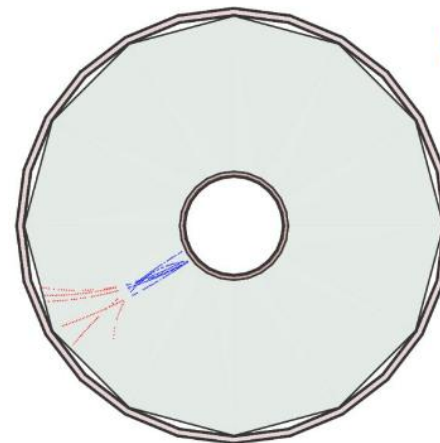
## • New designed insertion tooling

- Removal and insertion of inner sectors

## • Replace all 24 inner sectors

- 2018: One sector has been installed and used in the physics run
- Full installation in autumn 2018

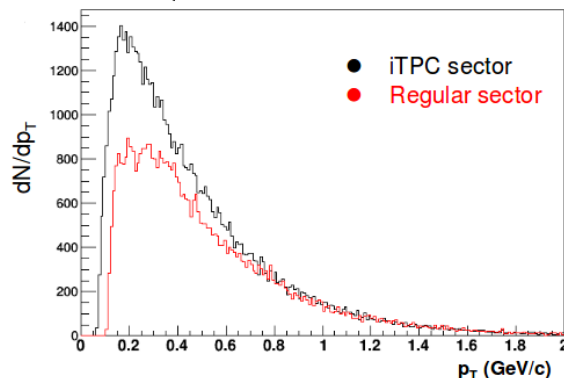
## iTPC (one sector) performance in the current isobar collisions



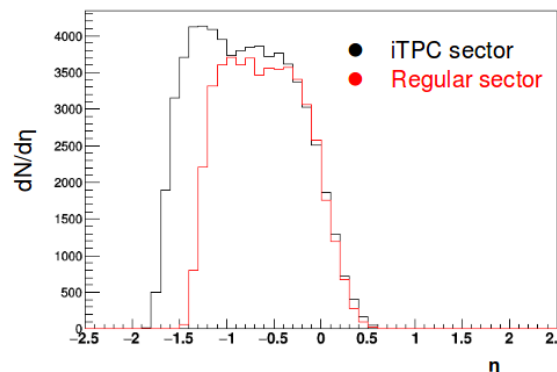
Event display

- Maximum hits per track: 45→72
- Lower transverse momentum threshold of 60 MeV/c
- $\eta$  coverage extended by 0.4 units

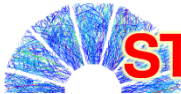
$p_T$  distributions - negative particles



$\eta$  distributions - negative particles



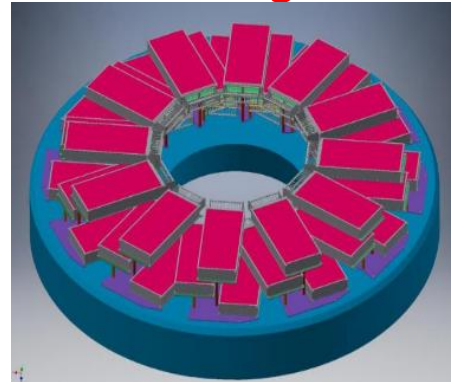
- **Install, commission and use 10% of the CBM TOF modules in STAR**
- **Design concept**
  - 3 layers, 12 sectors, 36 modules, 108 MRPCs
- **Provides PID in the forward direction**
  - Extended rapidity and yields
- **One sector with three modules has been installed for runs in 2018**
- **Full installation in autumn 2018**



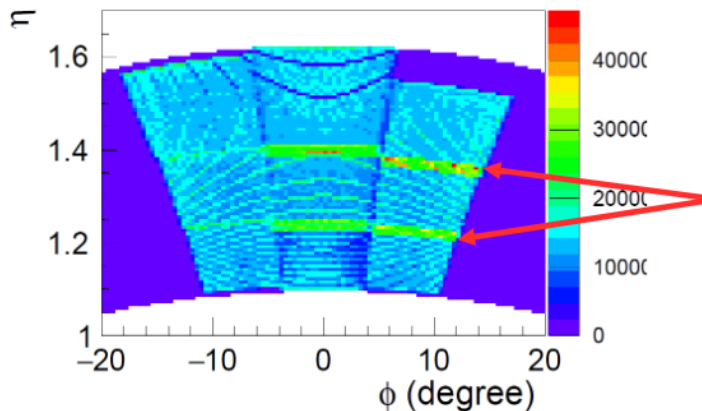
# STAR ☆ The endcap Time-Of-Flight

- Install, commission and use 10% of the CBM TOF modules in STAR
- Design concept
  - 3 layers, 12 sectors, 36 modules, 108 MRPCs
- Provides PID in the forward direction
  - Extended rapidity and yields
- One sector with three modules has been installed for runs in 2018
- Full installation in autumn 2018

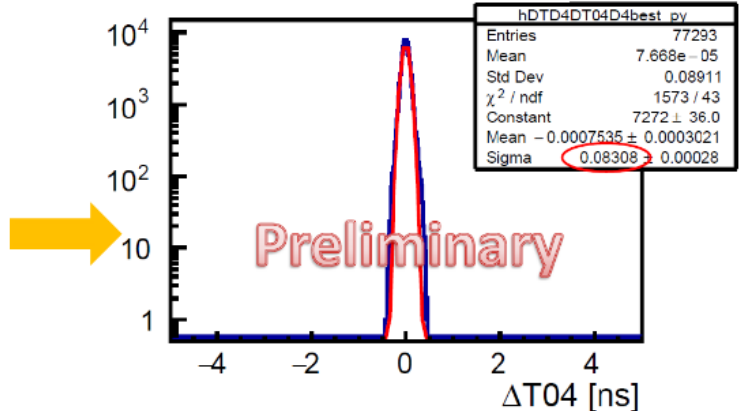
**eTOF (three modules) commissioned, integrated and participated in data taking**



- Reasonable  $\eta$ - $\phi$  hit distribution
  - eTOF works properly
- Time resolution 59 ps



**Overlap range of two MRPCs**

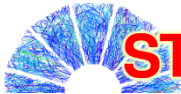


- ✓ System time resolution: 83 ps
- ✓ Counter time resolution: 59 ps

## Event Plane Detector

- **2 wheels**
  - East and West EPD ( $2.1 < |\eta| < 5.1$ )
- **12 super sectors**
  - Scintillator wedges, milled to form 31 tiles
  - Optically separated by epoxy
- **Fiber optics**
  - Wavelength-shifting fibers
  - Grouped in 3D-printed connectors
- **Sensors**
  - Silicon Photon Multipliers (SiPM)

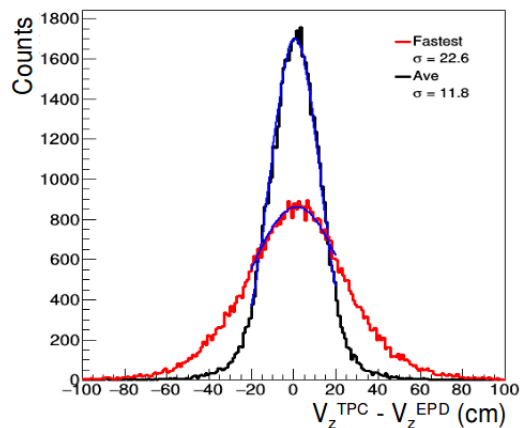
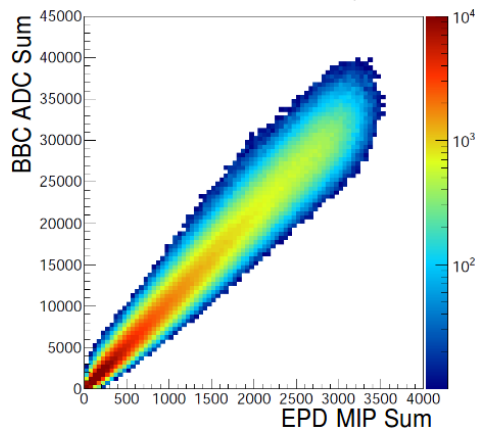




# STAR ☆ The Event Plane Detector

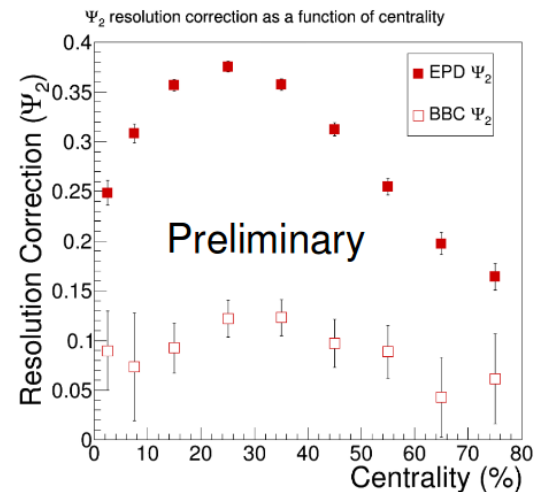
## Event Plane Detector

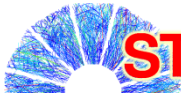
- **2 wheels**
  - East and West EPD ( $2.1 < |\eta| < 5.1$ )
- **12 super sectors**
  - Scintillator wedges, milled to form 31 tiles
  - Optically separated by epoxy
- **Fiber optics**
  - Wavelength-shifting fibers
  - Grouped in 3D-printed connectors
- **Sensors**
  - Silicon Photon Multipliers (SiPM)



## EPD is fully installed and took part in data taking in 2018

- All 744 tiles are good
- Good correlation between BBC and EPD
  - Correct timing
- **Timing resolution is about 0.75 ns** with fastest TAC method
  - 0.35 ns with average TAC method, raw slewing correction
- The 2<sup>nd</sup>-order event plane resolution is 0.37 in 20-30% central events at top energy isobar collisions





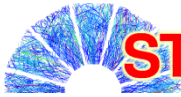
# STAR ☆ Short term plan

## Year 2018:

- Took ~1.5B events for Zr+Zr and Ru+Ru collision systems each
- Au+Au data at 27 GeV (~500M events) and 3.0 GeV (~300M events)
- ✓ Physics goals: Chiral Magnetic Effect, global polarization, dileptons, etc..

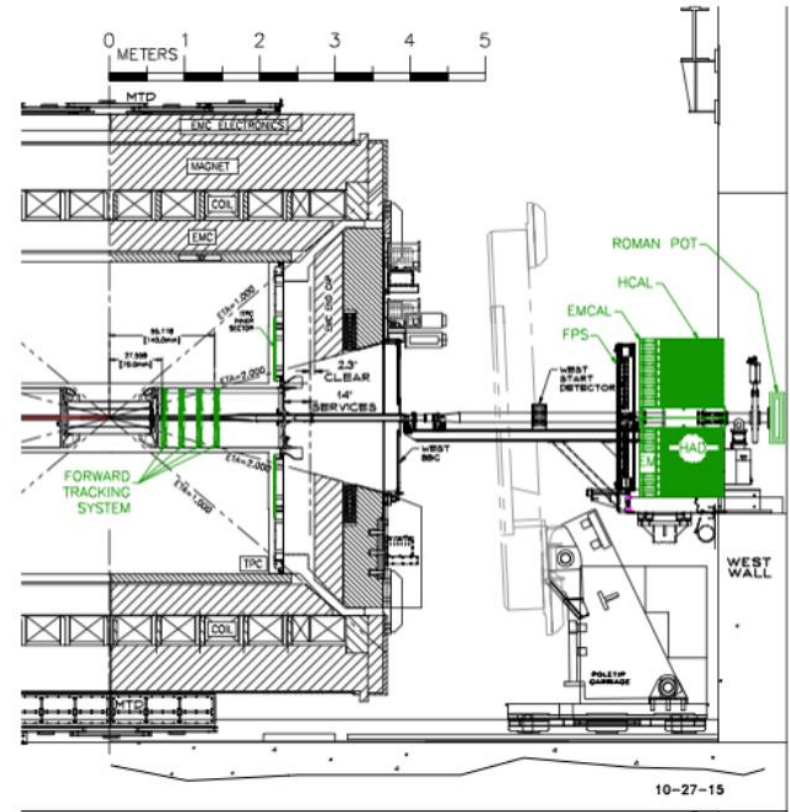
## Plan for 2019-2021:

Beam Energy (GeV/nucleon)	$\sqrt{s_{NN}}$ (GeV)	$\mu_B$ (MeV)	Run Time	Number Events
9.8	19.6	205	4.5 weeks	400M
7.3	14.5	260	5.5 weeks	300M
5.75	11.5	315	5 weeks	230M
4.55	9.1	370	9.5 weeks	160M
3.85	7.7	420	12 weeks	100M
31.2	7.7 (FXT)	420	2 days	100M
19.5	6.2 (FXT)	487	2 days	100M
13.5	5.2 (FXT)	541	2 days	100M
9.8	4.5 ( FXT)	589	2 days	100M
7.3	3.9 (FXT)	633	2 days	100M
5.75	3.5 (FXT)	666	2 days	100M
4.55	3.2 (FXT)	699	2 days	100M
3.85	3.0 (FXT)	721	2 days	100M



# STAR ☆ STAR Forward Upgrade

- STAR is proposing to install a Forward Calorimeter System (FCS), including an electromagnetic calorimeter and a hadron calorimeter, and a Forwarding Tracking System (FTS) in 2021+.
- Di-jet measurements with one or both jets in the forward region ( $2.8 < \eta < 3.7$ ) will be one of the highlights of this upgrade.
- FCS will provide gluon polarization at very low  $x$ 
  - $x \sim 5 \times 10^{-3}$  with FCS-EEMC di-jets
  - $x \leq 10^{-3}$  with FCS-FCS di-jets



10-27-15

- Collective dynamics and correlations
  - $v_1$ , longitudinal flow decorrelation, femtoscopy
- Particle production
  - Ultra-peripheral collisions, (anti)hypertriton,  $\Lambda_c$ ,  $\mathcal{N}(1S, 2S+3S)$
- High-pT particles and jet
  - $R_{CP}$  from BES-I, di-jet imbalance
- The STAR fixed-target results
- Detector upgrades